

30 **INTRODUCTION:**

31 Vertebrate gonadal sex differentiation is a unique process whereby the embryonic gonadal
32 primordium typically adopts either an ovarian or testicular fate (Brennan and Capel, 2004, Stevant
33 and Nef, 2019, Rotgers et al., 2018). This process involves the expression of sexually dimorphic
34 genes that activates one pathway and represses the other, making testis and ovary formation
35 mutually exclusive (Kim et al., 2006, Li et al., 2017). The undifferentiated gonad initially
36 comprises the same set of uncommitted cell lineage precursors; so-called supporting cells,
37 steroidogenic progenitors, germ cells and some other less well-defined cells (Lin et al., 2017, Lin
38 and Capel, 2015, Nef et al., 2019). The first cell lineage to differentiate is the supporting cell
39 lineage, giving rise to Sertoli cells in the male gonad and pre-granulosa cells in females (Niu and
40 Spradling, 2020, Chen et al., 2017, Zhang et al., 2015a). These cells are then thought to direct other
41 lineages down the testicular or ovarian pathways, respectively (Lin and Capel, 2015, Rotgers et
42 al., 2018, Wear et al., 2017, Gustin et al., 2016). In males, Sertoli cells organize into testis cords
43 and signal to neighboring steroidogenic precursors to become sex steroid-hormone producing fetal
44 Leydig cells in the developing testis (Yao et al., 2002). The same lineage gives rise to thecal cells
45 in the developing ovary, although this requires interactions with the germ cells (Liu et al., 2015,
46 Stevant et al., 2019). Germ cells themselves follow a fate governed by signals from the somatic
47 component of the gonad, giving rise to spermatogonia in the testis and oogonia in the ovary
48 (Barrios et al., 2010, Bowles et al., 2010, DiNapoli et al., 2006, Spiller et al., 2017). Other cell
49 types in the embryonic gonad are less well characterized, including the gonadal surface epithelium
50 (the source of the supporting and some of the steroidogenic cell lineages in mouse) and non-
51 steroidogenic “interstitial” cells derived from the surface epithelium or the adjacent mesonephric
52 kidney (DeFalco et al., 2011, Rotgers et al., 2018, Svingen and Koopman, 2013, Stevant and Nef,
53 2019).

54 Gonadal sex differentiation has been widely studied as a paradigm for the molecular genetic
55 regulation of development. In the mouse model, Y chromosome linked *Sry* gene initiates the testis
56 developmental program (Koopman et al., 1991, Sinclair et al., 1990, Hacker et al., 1995,
57 Kashimada and Koopman, 2010). It activates the related *Sox9* gene, leading to Sertoli cell
58 differentiation, and subsequent downstream signaling to channel other cell types down the male
59 pathway (Sekido et al., 2004, Sekido and Lovell-Badge, 2008, Qin and Bishop, 2005, Li et al.,

60 2014, Gonen et al., 2017). In mouse, once *Sry* has activated *Sox9*, the latter can drive complete
61 testis formation (Qin and Bishop, 2005), through activation of *Fgf9* signaling and other
62 mechanisms (Vidal et al., 2001, Kim et al., 2007, Gonen and Lovell-Badge, 2019, Schmahl et al.,
63 2004, Colvin et al., 2001). In female mammals (genetically XX), the absence of *Sry* allows
64 activation of the signaling molecule R-Spondin1, *Wnt4*, and stabilization of β -catenin, and
65 downstream expression of the transcription factor, *Foxl2* (Li et al., 2017, Parma et al., 2006,
66 Tomizuka et al., 2008, Maatouk et al., 2008, Chassot et al., 2008, Jordan et al., 2003). This engages
67 the ovarian pathway. Genetic antagonism exists throughout these opposing testis and ovarian
68 pathways; *Fgf9* (male) vs *Wnt4* (female), for example, and *Sry* vs R-Spo1 (Kim et al., 2006,
69 Lavery et al., 2012, Lau and Li, 2009). However, the molecular regulation of gonadal sex
70 differentiation is still incompletely understood, specifically with regard to cell types other than the
71 key supporting cell lineage. Recently, bulk and single-cell RNA sequencing approaches have
72 expanded the list of genes implicated in gonadal sex differentiation (Stevant et al., 2019, Stevant
73 et al., 2018, Estermann et al., 2020). Many novel genes uncovered by these approaches remain to
74 be functionally analyzed.

75 Our understanding of vertebrate gonadal development has been enhanced through comparative
76 studies in non-mammalian models. While several core genes required for gonadal sex
77 differentiation are conserved across species (*Sox9* in the testis and *Foxl2* in the ovary, for example)
78 (Kent et al., 1996, Major et al., 2019, Capel, 2017), upstream master sex genes can be divergent.
79 *Sry* is absent on non-mammals, and so other master sex triggers must exist. Among egg-laying
80 vertebrates, the transcription factor *DMRT1* plays a major role, analogous to *Sry*. *DMRT1* acts as
81 a master sex switch in birds and in many reptiles with temperature dependent sex determination,
82 inducing testis development (Smith et al., 2009, Ioannidis et al., 2020, Sun et al., 2017, Lambeth
83 et al., 2014). The chicken embryo, in particular, has proved valuable insights in the genetic
84 reregulation of gonadal sex differentiation, the evolution of genetic sex switches, and the cell
85 biology of gonadogenesis (Sekido and Lovell-Badge, 2007, Guioli et al., 2020, Smith and Sinclair,
86 2004, Estermann et al., 2020). As embryonic development occurs *in ovo* and is accessible for
87 experimental manipulation, the chicken provides a powerful model for functional analysis of
88 gonadal sex-determining genes (Schmid et al., 2015). This model has been particularly useful for
89 elucidating the cellular events underpinning gonad formation. Chickens have a ZZ male; ZW
90 female sex chromosome system, in which Z-linked *DMRT1* gene operates as a master testis

91 regulator via a dosage mechanism (two doses in males) (Ioannidis et al., 2020). In ZZ embryos,
92 the gonads differentiate into bilateral testes. As in mammals, the seminiferous cords form in the
93 inner gonadal medulla in chicken, comprising Sertoli that enclose germ cells (Smith and Sinclair,
94 2004). The male germ cells undergo mitotic arrest, entering meiosis only after hatching (Ayers et
95 al., 2013). In the female chicken gonad, the inner medulla is the site of aromatase gene expression.
96 Aromatase catalyzes the synthesis of estrogens, which are essential for ovarian differentiation in
97 birds (and other egg laying vertebrates) (Scheib, 1983, Vaillant et al., 2001b, Pieau and Dorizzi,
98 2004).

99 The avian model is particularly useful for shedding light on the role of the gonadal surface
100 epithelium. In mouse, the surface epithelium gives rise to the supporting cell lineage and then
101 contributes to the steroidogenic lineage (Lin et al., 2017, Stevant et al., 2018, Stevant et al., 2019).
102 In chicken, the surface epithelium gives rise to non-steroidogenic interstitial cells, not the
103 supporting cell lineage as in mouse (Estermann et al., 2020, Sekido and Lovell-Badge, 2007). Prior
104 to gonadal sex differentiation in chicken, the left gonadal epithelial layer is thicker than that the
105 right one (in both sexes) (Omotehara et al., 2017, Guioli et al., 2014). During sex differentiation,
106 this asymmetry becomes less marked in males (Guioli et al., 2014). However, symmetry is
107 maintained and becomes very pronounced in females (Smith and Sinclair, 2004). The right gonad
108 regresses in female birds, whereas the epithelium of the left gonad continues to proliferate to
109 become a thickened cortex (Guioli et al., 2014). Increased proliferation in the left cortex, rather
110 than increased apoptosis in the right cortex, is primarily responsible for the observed asymmetric
111 cortical development (Ishimaru et al., 2008). The left cortex is critical to ovarian development in
112 the avian model. The thickened left cortex contains both somatic cells and proliferating germ cells
113 that enter meiosis to later arrest at prophase I (Ukeshima, 1996). Immediately beneath the cortex
114 of the left ovary, interstitial medullary cells form a compact region called the juxtacortical medulla
115 (JCM). We have previously shown through single-cell RNA-seq that the cells of the JCM are non-
116 steroidogenic and derive from the ovarian surface epithelium (Estermann et al., 2020). The
117 functional significance of the JCM is unclear, although at later stages it expresses enzymes
118 involved in retinoic metabolism, and retinoic acid is implicated in cortical germ cell meiosis (Smith
119 et al., 2008).

121 We previously conducted bulk RNA-sequencing to identify novel genes involved in development
122 of the chicken ovary (Ayers et al., 2015). This screen identified *TGIF1* (*TGF- β Induced Factor*
123 *Homeobox 1*). *TGIF1* encodes a homeobox transcription factor that belongs to the superfamily of
124 TALE homeodomain proteins known to control many developmental processes, including
125 gastrulation, cell proliferation, and differentiation (Wotton et al., 1999a, Wotton et al., 1999b,
126 Lorda-Diez et al., 2009, Melhuish and Wotton, 2000, Wotton et al., 2001, Liu et al., 2014, Powers
127 et al., 2010). It has not previously been associated with gonadal sex differentiation in any species.
128 In the current study, we describe the role of *TGIF1* in chicken ovarian development. *TGIF1* is
129 specifically upregulated in female gonads at the onset of sexual differentiation, expressed in
130 cortical and pre-granulosa cells and is associated with the ovarian phenotype. Over-expression and
131 knockdown of *TGIF1* show that it is required for the formation of the female cortex and the
132 juxtacortical medulla. The data suggest that *TGIF1* is required for proper ovarian development in
133 the avian model, acting downstream of estrogen signaling.

134

135 **RESULTS**

136 ***TGIF1* but not *TGIF2* shows sexually dimorphic expression in embryonic chicken gonads.**

137 *TGIF1* was firstly identified as a candidate gene in avian gonadal sex differentiation from a
138 gonadal RNA-seq performed in our laboratory (Ayers et al., 2015). Differential expression analysis
139 showed that *TGIF1* mRNA expression was significantly higher in female compared to male gonads
140 at the onset of sex differentiation (Embryonic day (E6)/ HH stage 29) (Fig. 1A). *TGIF1* qRT-PCR
141 was performed on male and female gonads before (E4.5), during (E6.5) and after (E8.5) gonadal
142 sex differentiation to validate sexually dimorphic expression. Quantitative RT-PCR showed a
143 significant increase in *TGIF1* expression in female gonads from the onset of sexual differentiation
144 (E6.5-E8.5) (Fig. 1B), consistent with the RNA-seq. *TGIF1* was also expressed in male gonads,
145 but at consistently lower levels. *TGIF1* has a paralogue, *TGIF2*, with which it shares spatial and
146 temporal expression in other developmental contexts (Shen and Walsh, 2005). *TGIF2* expression
147 was not sexually dimorphic in the gonad RNA-seq data (Fig. S1A). This data was also confirmed
148 by qRT-PCR (Fig. S1B).

149

150 ***TGIF1* is expressed in the ovarian cortical and medullary pre-granulosa cells.**

151 For spatial expression analysis of *TGIF1*, whole mount *in situ* hybridization was performed on
152 male and female gonads at different developmental timepoints; before (E4.5/stage 24), during
153 (E6.5/stage 30) and after (E8.5/ stage 34) sexual differentiation. *TGIF1* mRNA expression was
154 stronger in female compared than male gonads from E6.5 / HH stage 30 (Fig. 1C), consistent with
155 the RNA-seq and qRT-PCR results. In developing ovaries, *TGIF1* mRNA was localized in the
156 cortex and in the medulla (Fig. 1D). In males, expression was detected at the surface epithelium at
157 E6.5, though weaker than in the developing ovary (Fig. 1D). After the onset of sexual
158 differentiation at E8.5 in males, weak expression was detected in the seminiferous cords of the
159 medulla.

160 The developing chicken ovary comprises two distinct compartments: the outer cortex, which
161 becomes thickened in the left ovary and is the site of oogenesis, and an inner medulla comprising
162 interstitial, supporting and steroidogenic cells (Smith and Sinclair, 2004, Estermann et al., 2020).
163 Co-localization with specific markers was performed to determine the cell types expressing *TGIF1*
164 in the ovary. Aromatase and cytokeratin immunofluorescence were performed following *TGIF1*
165 *in situ* hybridization on tissue sections (Fig. 2). Aromatase marks estrogenic pre-granulosa cells,
166 while cytokeratin marks cortical cells. In the left ovary, *TGIF1* was expressed in the cortical cells,
167 colocalizing with cytokeratin. Lack of *TGIF1* expression in the right female gonad corresponded
168 with the lack of a proliferating cortex. *TGIF1* mRNA also co-localized with the medullary pre-
169 granulosa marker, aromatase, in both left and right gonads. *TGIF1* was not expressed in the
170 interstitial cells between medullary cords nor in the juxtacortical medulla of female gonads (Fig.
171 2). In summary, *TGIF1* expression was restricted to cortical and pre-granulosa cells, both key cell
172 types in ovarian development and differentiation.

173

174 ***TGIF1* expression is sensitive to estrogens:**

175 Ovarian differentiation in birds is regulated by estrogen, catalyzed by the female restricted enzyme
176 aromatase. *In ovo* injection of 17 β -estradiol (E2) or the aromatase inhibitor fadrozole cause
177 feminization and masculinization of the gonads, respectively (Bannister et al., 2011, Guioli et al.,
178 2020). To determine whether *TGIF1* is responsive to estrogen signaling during ovarian

179 development, sex reversal experiments were conducted. *TGIF1* was assayed following
180 masculinization of female embryos with fadrozole, which inhibits aromatase enzyme action, or by
181 applying estrogen to male embryos to induce feminization. *TGIF1 in situ* hybridization was
182 performed in E9.5 male and female urogenital system (UGS) treated with 17- β -estradiol (E2) or
183 vehicle (Control) at E3.5 (Fig. 3). Male gonads treated with E2 were morphologically feminized,
184 with female-like asymmetry, characterized by a larger left and smaller right gonad. These gonads
185 also showed structural organization typical of an ovary, with a thickened cortex (cytokeratin
186 positive), aromatase positive pre-granulosa cells in the medulla and downregulated expression of
187 the testis marker, anti-Müllerian hormone (AMH) (Fig. 3). *TGIF1* expression was upregulated in
188 males treated with E2, compared with the vehicle control, showing a similar expression pattern to
189 females (Fig. 3).

190 Female gonads treated with the aromatase inhibitor (AI) were masculinized, as expected. Female-
191 type gonadal asymmetry was markedly reduced, and gonads showed testicular like morphology,
192 containing AMH positive testicular cords, and a reduced cortex and reduced aromatase positive
193 cells (Fig. 4A). *TGIF1* expression was also reduced in female gonads treated with aromatase
194 inhibitor, consistent with the gonadal sex reversal (Fig. 4A). To quantify this change, *TGIF1* qRT-
195 PCR was performed in E8.5 male and female gonads exposed to AI or vehicle (Control).
196 Consistent with the *in situ* hybridization data, female gonads treated with AI showed a significant
197 reduction of *TGIF1* expression in comparison with the vehicle control (Fig. 4B). Altogether, these
198 results indicate that *TGIF1* mRNA expression responds to estrogens during ovarian differentiation
199 in the chicken embryo.

200

201 ***TGIF1* over-expression in left testis results in gonadal feminization.**

202 To examine the effects of *TGIF1* over-expression *in ovo*, electroporation of DNA constructs was
203 used. Gonadal epithelial cells can be specifically targeted by performing electroporation of plasmid
204 DNA into the coelomic epithelium at E2.5 without effecting the underlying medullary cord cell
205 population (Estermann et al., 2020). This method allows insight into the role of *TGIF1* specifically
206 in the ovarian epithelium/cortex. *TGIF1* open reading frame was cloned into TOL2-CAGGS-GFP
207 vector, which, in presence of the transposase, integrates into the genome, stably expressing *TGIF1*
208 and GFP in the targeted and daughter cells (Sato et al., 2007). The ability of this construct to

209 overexpress TGIF1 was assayed in vitro in the DF1 chicken fibroblastic cell line. Cells transfected
210 with TGIF1 overexpressing plasmid significantly expressed around 30 times more TGIF1 than the
211 empty plasmid (GFP control) (Fig. S1C).

212 TOL2-CAGGS-GFP-T2A-TGIF1 (TGIF1 OE) or TOL2-CAGGS-GFP (GFP Control) plasmid
213 were co-electroporated with a plasmid expressing transposase into the left coelomic epithelium at
214 E2.5 (stage 14). Embryos were collected at E8.5, sexed and immunofluorescence was performed
215 against different gonadal markers. Figure 5 and 6 show the results of these experiments in which
216 TGIF1 was over-expressed in the gonadal cortex of male embryos. In the absence of a suitable
217 antibody to detect TGIF1 in chicken, GFP was used as a marker of electroporation. As expected,
218 GFP was detected in the gonadal cortical/epithelial cells (Fig. 5), and in the interstitial cells that
219 they generate, but not in supporting cells in males (Fig. 6) and females (Fig. S2). When *TGIF1*
220 was over-expressed in female gonads, no structural or expression difference with the control was
221 found (Fig. S2). In contrast, TGIF1 overexpression in left male gonads resulted in a change in the
222 epithelial cell structure (cytokeratin positive, fibronectin negative), resembling cuboidal rather
223 than squamous epithelium that is typical of the testis (Fig. 5A). Image quantification analysis
224 indicated that TGIF1 over-expression resulted in a significant increase of the gonadal epithelial
225 area (Fig. 5C) and the thickness of the epithelium (cell height) (Fig. 5C). In addition, an increment
226 of cytokeratin positive mesenchymal cells was detected, suggesting augmentation of an epithelial
227 to mesenchyme transition (EMT) (Fig. 5A). In male gonads overexpressing *TGIF1*, interstitial
228 cells derived from the coelomic epithelial cells by EMT (GFP⁺, fibronectin⁺) accumulated
229 underneath the epithelial layer, forming dense clusters (Fig. 6A). This accumulation of interstitial
230 cells resembles the organization of the ovarian juxtacortical medulla (JCM) and resulted in a
231 displacement of the testicular cords (AMH⁺) towards the more basal region of the gonad (Fig. 6B).
232 Image quantification analysis indicated that TGIF1 over-expression resulted in a significant
233 increase in the juxtacortical medulla area, compared with the controls (Fig. 6C).

234 To examine its effects on the gonadal medulla, TGIF1-GFP was over-expressed using the
235 RCASBP viral vector. Unlike TOL2, this vector can spread horizontally to neighboring cells. This
236 is important, as it can deliver transgenic expression to the medullary cord population which cannot
237 be targeted by TOL2 electroporation. *TGIF1* ORF was cloned into RCAS(A)-GFP viral vector.
238 RCAS(A)-GFP-T2A-TGIF1 (TGIF1 OE) or RCAS(A)-GFP (GFP Control) plasmids were

239 electroporated in E2.5 left coelomic epithelium. Urogenital systems were collected at E7.5-E8.5,
240 sexed and immunofluorescence was performed against different gonadal markers. Over-
241 expression of TGIF1 in male gonads using this approach did not alter the testicular development.
242 Supporting cells developed normally, AMH, SOX9 and DMRT1 expression was similar than the
243 control gonads (Fig. S3), and no female markers (aromatase or FOXL2) were detected (data not
244 shown). Instead, the same morphological changes were detected when TGIF1 was overexpressed
245 only in the coelomic epithelial cells: displacement of the supporting cells from the sub-epithelial
246 region (Fig. S3A and B) and an increased thickness of the gonadal surface epithelium, marked by
247 diagnostic cytokeratin staining. The cells of the epithelium adopted a female-like cuboidal
248 morphology instead of the squamous epithelium typical of the testis (Fig. 6). Altogether, this data
249 suggests that TGIF1 miss-expression does not impact Sertoli cell differentiation in chicken gonads.

250

251 **Ovarian TGIF1 knock down inhibits gonadal cortex and juxtacortical medulla formation**

252 *In ovo* gene knockdown was performed to assess the role of TGIF1 during cortical and juxtacortical
253 medulla formation in the developing ovary. Four different shRNAs were designed against the
254 *TGIF1* open reading frame and were cloned into the retroviral vector RCASBP (D) carrying a blue
255 fluorescent protein (BFP) reporter. These were screened for knockdown efficiency *in vitro* using
256 the DF1 chicken fibroblastic cell line. DF1 cells were transfected with plasmids carrying BFP-
257 T2A and a non-silencing control shRNA (NS shRNA), or one of four different shRNAs designed
258 for TGIF1 knockdown. After all cells became BFP positive, they were transfected with TOL2
259 plasmid over-expressing chicken TGIF1-GFP (TOL2-GFP-T2A-TGIF1). Plasmid expressing
260 mCherry was used as a transfection control. 48 hours post transfection, cells were fixed, and GFP
261 fluorescence was quantified as a measure of *TGIF1* knockdown (Fig. 8A). All of the shRNAs
262 showed a significant decrease of GFP intensity. Sh988 showed the strongest inhibition (66%),
263 followed by sh364 (57%), sh416 (46%) and sh318 (16%). These values were calculated using the
264 mean of each group using NS shRNA as a control (100%) (Fig. 8B).

265 TGIF1 sh998 was cloned into a TOL2 vector expressing nuclear BFP. TOL2-TGIF1sh998-nBFP
266 or TOL2-NSshRNA-nBFP were *in ovo* co-electroporated with TOL2-ACAGS-GFP
267 (electroporation reporter) and transposase expressing plasmid into the left coelomic epithelium at
268 E2.5. Urogenital systems were collected at E8.5, genetically sexed by PCR and

269 immunofluorescence was performed for different gonadal markers. *TGIF1* knock down resulted
270 in a substantial size reduction of the targeted left ovaries, in comparison with the controls
271 electroporated with NS shRNA. Aromatase positive pre-granulosa cells were still present in the
272 gonadal medulla (Fig. 9A) and no Sertoli cell markers (SOX9, AMH, DMRT1) were up-regulated
273 (data not shown). Strikingly, an ovarian cortex was absent in the female *TGIF1* knock down
274 gonads, as revealed by cytokeratin expression (Fig. 9B). Instead, the epithelial cells exhibited a
275 flattened morphology similar to the right gonadal epithelium or the testicular epithelium (Fig. 9B).
276 In addition, these ovaries lacked a clear juxtacortical medulla (JCM), evidenced by the absence of
277 condensed fibronectin positive cells in between the epithelium and the aromatase positive pre-
278 granulosa cells (Fig. 9C). Due to the absence of a defined cortex, the germ cells remained in the
279 medulla (similar to their fate in the right gonad) (Fig. 9D). Altogether, these results indicate that
280 *TGIF1* is necessary to develop an ovarian cortex. Moreover, *TGIF1* is the first gene reported to be
281 required for the juxtacortical medulla formation.

282

283 **DISCUSSION:**

284 Gonadal sex differentiation provides an ideal model for studying progressive cell fate decisions
285 (Lin and Capel, 2015, Munger and Capel, 2012). During gonadal morphogenesis, cell lineages
286 differentiate into ovarian or testicular cell types. The first cells to differentiate are the supporting
287 cells (Sertoli cells in males, pre-granulosa cells in females) (Nef et al., 2019). These cells then
288 signal to control differentiation of the other gonadal lineages, including steroidogenic and non-
289 steroidogenic cells, and they also influence germ cell fate (spermatogonia in males, oogonia in
290 females) (Stevant et al., 2019, Stevant and Nef, 2019). Due to the central role of the supporting
291 cell population, most research in the field has focused on the granulosa vs Sertoli cell fate decision.
292 Less is understood about the development and role of the gonadal surface (coelomic) epithelium.
293 However, lineage tracing and single-cell RNA-seq have shown that this gonadal compartment has
294 significantly different roles in mammalian versus avian models. In the mouse embryo, the surface
295 epithelium is central to gonadal differentiation. This layer of cells is the source of most somatic
296 cell progenitors in the embryonic murine gonad (DeFalco et al., 2011, Nicol and Yao, 2014). The
297 surface epithelial cells express the transcription factors *Wt1*, *Gata4* and *Sfl*, they proliferate to
298 first give rise first to the supporting cell lineage, and, subsequently, at least some of the

299 steroidogenic population (Hatano et al., 2010, Karl and Capel, 1998, Stevant and Nef, 2019,
300 Stevant et al., 2019, Nef et al., 2019). Somatic cells of the surface epithelium in mouse divide
301 asymmetrically, producing one daughter cell that remains at the surface and one that undergoes an
302 epithelial to mesenchyme transition (EMT), ingressing into the gonad. This process is regulated
303 by Notch signaling, via the antagonist, Numb (Lin et al., 2017). Homeobox transcription factors
304 such as *Emx2*, *Six1* and *Six4* contribute to this EMT (Kusaka et al., 2010, Fujimoto et al., 2013).
305 In contrast to mouse, lineage tracing in the chicken embryo clearly shows that proliferating surface
306 epithelium gives rise to non-steroidogenic interstitial cells, not the supporting cell lineage (which
307 derives from mesonephric mesenchyme) (Sekido and Lovell-Badge, 2007, Estermann et al., 2020).
308 Furthermore, epithelial cells differentiate into a stratified layer of cortical cells in the left female
309 gonad, whereas this process does not occur in males (Estermann et al., 2020). The development of
310 a thickened left gonadal cortex is critical for proper ovary formation and female reproduction in
311 birds. Germ cells accumulate in the ovarian cortex during embryonic stages and are signaled to
312 enter meiotic prophase (Smith et al., 2008). After hatching, germ cells development proceeds as
313 the cortex is the site of folliculogenesis in avians (Johnson and Woods, 2009, Li et al., 2016, Hu
314 et al., 2021). The importance of the cortex is revealed by the asymmetry of female avian gonadal
315 development. The right gonad fails to elaborate as cortex in females and germ cells remain in the
316 medullar, where they eventually become atretic (Guioli et al., 2014) .

317 The results presented here demonstrate that the TALE homeobox gene, *TGIF1*, plays a key role in
318 development of the gonadal cortex in the chicken embryo. This gene is upregulated during female
319 but not male gonads development (Fig. 1). It is strongly expressed in the female gonadal surface
320 epithelium at onset of sexual differentiation (E6.5/stage 30), and in the gonadal medulla. Targeted
321 over-expression in the male surface epithelium induces a thickened cortex, while targeted
322 knockdown in in females blocks proper cortical layer development. Manipulation of expression in
323 the medulla did not have an overt effect upon gonadogenesis. Furthermore, *TGIF1* expression was
324 responsive to modulation of estrogen, which is essential for ovarian development in birds (Scheib,
325 1983, Elbrecht and Smith, 1992, Vaillant et al., 2001a). Inhibition of the estrogen-synthesizing
326 enzyme, aromatase, resulted in down-regulation of *TGIF1* expression (Fig. 4). This indicates that
327 *TGIF1* is a downstream target of estrogen, either directly or indirectly, during ovary formation. In
328 the chicken embryo, two roles are ascribed to the estrogen that is synthesized by medullary cords
329 cells of female embryos at the onset of gonadal sex differentiation. Firstly, estrogen acts in the

330 medulla itself to antagonize the induction of the testis factors, DMRT1 and SOX9 (Smith et al.,
331 2003, Ioannidis et al., 2021). Secondly, acts on the surface epithelium in a paracrine fashion, where
332 it stimulates development of the gonadal cortex (Gasc and Stumpf, 1981, Wartenberg et al., 1992).
333 Correspondingly, estrogen receptor α (ER- α), is expressed in both gonadal compartments in chicken
334 embryos (Andrews et al., 1997, Gonzalez-Moran, 2014.) Exogenous estrogens can induce cortical
335 cell differentiation in embryonic male (ZZ) gonads (Guioli et al., 2020). While gonadal asymmetry
336 in the chicken is driven by asymmetric expression of *Pitx2* in the cortex (Rodriguez-Leon et al.,
337 2008, Guioli and Lovell-Badge, 2007), cortical cell proliferation is related to estrogen action. ER-
338 α is expressed in the left but not the right gonadal epithelium. This is consistent with the cortical
339 development in the left but not in the right gonad. RNAi or domain negative-mediated
340 downregulation of ER- α cause a reduction in cortical size, indicating that ER- α and estrogens are
341 essential for cortex formation (Guioli et al., 2020). Here, we found that *TGIF1* expression was
342 induced by estrogen and downregulated when estrogen synthesis was inhibited (Fig. 3 and 4).
343 Moreover, *TGIF1* and ER- α are both expressed the left gonadal epithelium (and in supporting cells
344 of the medulla), suggesting that estrogens, through ER α , could regulate *TGIF1* expression in
345 chicken ovaries. This would also explain why *TGIF1* is expressed in the left gonadal epithelium
346 but not in the right (Fig. 2). Similar to ER α , TGIF1 knock down in female gonads resulted in lack
347 of cortical development, despite the presence of estrogens (aromatase expression was not
348 perturbed). This indicates that *TGIF1* is required for ovarian cortical formation, acting downstream
349 of the estrogen signaling pathway. It will be of interest to examine the regulatory region of the
350 chicken TGIF1 gene for estrogen response elements.

351 The data presented here indicate that one of the functions of TGIF1 is the maintenance of columnar
352 epithelial cells the gonadal cortex. The epithelium in the left and right gonads in both males and
353 female chicken embryos at E6.5 shows an asymmetry, being thicker in the left than the right gonad
354 (Guioli et al., 2014). In females this structure continues proliferating, whereas in the male, it
355 flattens and to a squamous monolayer. *TGIF1* over-expression in males did not induce the
356 formation of a multilayered female like cortex. However, epithelial cell thickness was increased
357 (Fig. 5 and 6). This suggests that TGIF1 is required for maintaining columnar epithelial structure
358 and inhibiting a squamous phenotype. *Tgif1/Tgif2* double null mouse embryos display
359 disorganized epiblasts and lacked the typical columnar epithelial morphology (Powers et al.,

360 2010). This suggests that the role of TGIF1 in maintaining the epithelium structure may be a
361 conserved function during embryogenesis.

362 TGIF1 May be acting through a number of mechanisms to promote development of the ovarian
363 cortex in the chicken embryo. *TGIF1* encodes a homeodomain transcription factor of the TALE
364 family (Three Amino Loop Extension). At least three signaling pathways have been linked to
365 TGIF1 function; TGF (Wotton et al., 1999b), retinoic acid (Bertolino et al., 1995) and Wnt/ β -
366 catenin (Zhang et al., 2015b). All of these pathways are known to be engaged in the embryonic
367 gonads in chicken and in mouse. TGIF1 is a TGF- β signaling inhibitor, binding to phospho-Smad2,
368 recruiting histone deacetylases and acting as a co-repressor of Smad target genes (Wotton et al.,
369 1999a). Chicken ovaries exposed to TGF- β 1 display a reduction of somatic cells due to decreased
370 cell proliferation (Mendez et al., 2006). In addition, there is a reduction in the number of germ
371 cells in the cortex and an increased number in the medulla (Mendez et al., 2006). This suggests an
372 effect in the cortical compartment or in the capacity of germ cells to migrate. In mice, nodal, activin
373 and TGF- β signalize through Smad 2/3/4 and are key in testicular development, suppressing the
374 pre-granulosa program (Gustin et al., 2016, Wu et al., 2013). In contrast, BMP molecules such as
375 BMP2 signal through Smad 1/5/8 and are important for ovarian differentiation in mouse
376 (Kashimada et al., 2011). TGIF1, being expressed in the female supporting cells and cortex, could
377 act to repress the Smad 2/3 masculinizing signaling and allowing BMPs to induce ovarian
378 differentiation. Further research should explore the role of TGIF1 modulating the balance between
379 BMP vs TGF- β pathways in the gonadal context.

380 In chicken, lineage tracing experiments show that non-steroidogenic interstitial cells derive from
381 the gonadal surface epithelium by an EMT (Estermann et al., 2020). The ultimate fate of these
382 cells is poorly known, but they likely contribute to peritubular myoid cells in males but their role
383 in females is obscure. However, in the chicken, there is an accumulation of interstitial cells directly
384 underneath the cortex in females, forming a zone called the so-called juxtacortical medulla. This
385 structure is not present in testis, and its functional significance is not known. However, several
386 genes show restricted expression in the JCM later in development, such as CYP26B1, responsible
387 for retinoic acid degradation (Smith et al., 2008). Recently, TGIF1 was found to be expressed in
388 chicken dorsal neural tube and in delaminating cardiac neural crest, where it is required for the
389 formation of mesenchymal derivatives of the crest (Gandhi et al., 2020). In addition, TGIF1 is

390 associated with increased breast, lung and colorectal cancer migration and metastasis (Haider et
391 al., 2020, Xiang et al., 2015, Wang et al., 2017) and can activate the Wnt/ β -catenin signaling to
392 promote cancer cell proliferation and migration (Wang et al., 2017, Zhang et al., 2015b). TGIF1
393 over-expression in male coelomic epithelium induced fibronectin positive interstitial cells
394 accumulation underneath the gonadal epithelium, despite lacking a fully developed cortex (Fig.
395 5B). This process would appear to be independent estrogen signaling, due to the absence of
396 aromatase expression, and consequently, estrogens in the male gonads miss-expressing TGIF1.
397 Consistently, ovaries lacked a juxtacortical medulla when TGIF1 was knocked down (Fig. 9). This
398 indicates that TGIF1 induces EMT in the epithelial cells to generate interstitial cells, which
399 accumulate beneath the gonadal epithelium. TGIF1 is the first gene reported to be required for the
400 juxtacortical medulla formation. Interestingly, TGIF1 is expressed in the epithelial cells but not in
401 the interstitial cells, suggesting that TGIF1 is downregulated after the EMT, consistent with its
402 role of maintaining the surface epithelium.

403 TGIF1 was also found to be expressed in the pre-granulosa cells, colocalizing with aromatase (Fig.
404 2). This suggest that TGIF1 could play a role in supporting cell differentiation. SOX9 is a marker
405 of Sertoli cell, and it is known to have a role in repressing the female differentiation pathway and
406 inducing and maintaining the male genetic program. When TGIF1 was over-expressed in mouse
407 limb mesodermal micromass cultures, chondrogenic markers, such as Sox9, were downregulated
408 (Lorda-Diez et al., 2009). When TGIF1 was silenced, SOX9 expression was up-regulated,
409 suggesting a direct or indirect role of TGIF1 in inhibiting SOX9 (Lorda-Diez et al., 2009). Here,
410 over-expressing TGIF1 in testicular supporting cells did not result in a reduction of SOX9
411 expression or the upregulation of pre-granulosa markers (Fig. S3). This suggest that this role of
412 TGIF1 is not conserved among mouse and chicken or that its function differs between limbs and
413 gonads. The current data presented here indicate that TGIF1, by itself, has no role in early
414 differentiation of supporting cells in the chicken model.

415 TGIF1 and TGIF2 share similar spatial and temporal expression during embryonic development.
416 In addition, they have similar binding domains, suggesting functional redundancy (Shen and
417 Walsh, 2005, Powers et al., 2010). TGIF2 has redundant functions with TGIF1, but they need to
418 be co-expressed in the same cells in order to have a compensatory effect (Lee et al., 2015). In
419 chicken gonads, both TGIF1 and TGIF2 are expressed in the gonads, but RNA-seq data showed

420 that TGIF2 expression is lower than TGIF1 (Fig. 1A & S1A). In ovarian TGIF1 knock down
421 experiments, TGIF2 expression levels were not able to rescue the cortical and juxtacortical
422 formation. This suggest that in chicken gonads TGIF1 and TGIF2 do not share the same functions,
423 or they are not expressed in the same cell types. While TGIF1 not previously been linked to
424 vertebrate gonadal development, *Drosophila* TGIF and tammar wallaby TGIF2 are important for
425 spermatogenesis (Ayyar et al., 2003, Hu et al., 2011). In chicken, TGIF2 expression was not
426 sexually dimorphic. Due to the reported role in spermatogenesis, it would be interesting to study
427 TGIF2 expression in adult birds to identify if this function is conserved among species.

428 In summary, in chicken ovaries, the data presented here indicated that activation of the ER α
429 signaling pathway by estrogens induces the expression of TGIF1 in the gonadal epithelium of the
430 female the chicken embryo. TGIF1 expression supports development of the ovarian cortex,
431 inhibiting the epithelial flattening, and it induces formation of the juxtacortical medulla by
432 increased EMT (Fig. 10). In chicken testis, TGIF1 expression is not induced in the gonadal
433 epithelial cells due to the lack of estrogens and, consequently, ER α signaling. This results in the
434 epithelial flattening, inhibiting the formation of the juxtacortical medulla (Fig. 10). Our results
435 support the proposal that supporting cell differentiation and cortical sex differentiation are two
436 independent processes (Guioli et al., 2020, Ioannidis et al., 2021). This research introduces TGIF1
437 as one of the main regulators of cortical differentiation. In addition, we identified TGIF1 as the
438 first known regulator required for juxtacortical medulla formation and provide evidence that a fully
439 developed cortex or estrogens are not required for this process. Future research should focus on
440 the downstream targets of TGIF1 in regulating this process. In addition of its role as a transcription
441 factor, TGIF1 was also associated with several functions in signaling pathways. These includes
442 TGF- β , retinoic acid and WNT/ β -catenin pathways (Lorda-Diez et al., 2009, Liu et al., 2014,
443 Gongal and Waskiewicz, 2008, Castillo et al., 2010, Zhang et al., 2015b). A comprehensive
444 analysis of the role of TGIF1 in regulating cell signaling in the gonadal context is required to fully
445 understand its role in gonadogenesis. This could also shed light in the role of TGIF1 in the
446 supporting cell, which still remains unknown. Our research provides new insights in chicken
447 ovarian differentiation and development, specifically in the process of cortical and juxtacortical
448 medulla formation, a less explored field.

449 **MATERIALS AND METHODS:**

450 Eggs and samples:

451 Fertilized HyLine Brown chickens (*Gallus gallus domesticus*) eggs were obtained from Research
452 Poultry Farm (Victoria, Australia) and incubated under humid conditions at 37 °C. Gonads and
453 urogenital systems were collected at various time points throughout development and staged *in*
454 *ovo* according to Hamburger and Hamilton (Hamburger and Hamilton, 1951). PCR sexing was
455 performed as mentioned before (Clinton et al., 2001).

456 qRT-PCR:

457 Gonadal pairs were collected in Trizol reagent (Sigma-Aldrich) and kept at -80 degrees till
458 processing. After sexing, 3 gonadal pairs from the same sex were pooled for each sample,
459 homogenized and followed RNA extraction protocol by Phenol-Chloroform method as per the
460 manufacturer's instructions. Genomic DNA was removed from the RNA samples using DNA-
461 free™ DNA Removal Kit (Invitrogen) and 200-500 ug of RNA was converted into cDNA using
462 Promega Reverse Transcription System. qRT-PCR was performed using QuantiNova SYBR®
463 Green PCR Kit. Expression levels were quantified by Pfaffl method (Pfaffl, 2001) using β -actin
464 as housekeeping gene. Data was analyzed using multiple t-tests (one per embryonic stage or
465 treatment). Statistical significance determined using the Holm-Sidak. All used primers are listed
466 in Sup. table 1.

467 Whole mount *in situ* hybridization:

468 Whole mount *in situ* hybridization (WISH) was performed as previously described (Estermann et
469 al., 2020). At least three embryos were used for each stage and sex. Urogenital systems were
470 dissected and fixed overnight in 4% paraformaldehyde. Tissues were dehydrated in a methanol
471 series and stored till usage. Samples then were rehydrated to PBS plus 0.1% Triton X-100 before
472 digestion in proteinase K (1 ug/mL in PBS plus 0.1% Triton X-100) for 30 to 90 minutes at RT.
473 Tissues were then washed, briefly refixed, and incubated overnight at 65°C in (pre)hybridization
474 buffer. Digoxigenin-labeled antisense RNA probes were synthesized using a digoxigenin labeling
475 kit, according to the manufacturer's instructions (Life Technologies). TGIF1 probes (514 bp) were
476 cloned from gonadal cDNA using primers listed in Table S1. DNA sequences were cloned into

477 pGEM-T Easy vector and sequences were confirmed before use. For probe generation, a DNA
478 template was first generated by PCR amplification of the insert, using M13 forward and reverse
479 primers, encompassing RNA polymerase binding sites. Antisense and sense digoxigenin-labeled
480 RNA probes were generated using the relevant T7 or SP6 RNA polymerase sites present in the
481 amplified PCR product. Following synthesis, riboprobes were precipitated overnight at -20°C. For
482 each probe, 7.5 uL were added to 2 mL (pre)hybridization mix and incubated overnight at 65 °C.
483 Following low and high stringency washes, tissues were washed, preblocked, and incubated
484 overnight at 4 °C with alkaline phosphatase–conjugated anti-digoxigenin antibodies in TBTX
485 (1:2000; Roche). Following extensive washing in TBTX, tissues were exposed to chromogen
486 (NBT/BCIP) for up to 3 hours. For each gene, the color reaction was stopped at the same time by
487 rinsing in NTMT buffer, followed by washing in PBS and imaging. Tissues were then overstained
488 cryoprotected in PBS plus 30% sucrose, snap frozen in OCT embedding compound, and
489 cryosectioned between 14 and 18 um or 10 um if they were processed for immunofluorescence.

490 Sex reversal:

491 For masculinization, eggs were either injected with 1.0 mg of fadrozole (Novartis) in 100 uL of
492 phosphate-buffered saline (PBS) or injected with PBS alone at E3.5 as previously described (Hirst
493 et al., 2017a). For feminization 17β-estradiol (Sigma-Aldrich) was initially resuspended in 100%
494 Ethanol (10 mg/ul) and then diluted to 1 mg/ml in sesame oil. 100 ul of this 1 mg/ml solution (0.1
495 mg of E2) or a 10% Ethanol in Sesame oil solution (Vehicle) was injected into E3.5 eggs. Eggs
496 were incubated until day 9.5 of development (HH34) before processing them for whole mount *in*
497 *situ* hybridization.

498 TGIF1 overexpression construct design and electroporation

499 The Tol2 system was used to integrate TGIF1 overexpression construct into the genome of
500 electroporated cells in the chicken embryos (Kawakami, 2007; Sato et al., 2007). TGIF1 ORF was
501 amplified from gonadal cDNA using specific primers (See Table S1) and TA cloned into pT2-
502 aCAGS-GcT or RCAS(A)-aCAGS-GcT and sequenced. DF1 cell (ATCC) transfection with
503 TOL2-GFP-T2A-TGIF1 overexpression plasmid or control plasmid and transposase expressing
504 plasmid was performed following the Lipofectamine 2000 protocol (Life Technologies). Cells

505 were collected 48 hours post transfection and Trizol RNA extraction was performed as described
506 before.

507 *In ovo* electroporation of p-CAGGS-Transposase with pT2-aCAGS-GcT-T2A-TGIF1 (TGIF1
508 OE) or pT2-aCAGS-GcT (GFP Control) constructs was performed as previously described (Hirst
509 et al., 2017b) on E2.5 embryos, targeting the left coelomic epithelium. Embryos were harvested at
510 E7.5-E8.5, sexed and processed for immunofluorescence. For RCAS electroporation, RCAS(A)-
511 aCAGS-GcT-T2A-TGIF1 (TGIF1 OE) or RCAS(A)-aCAGS-GcT (GFP control) were
512 electroporated.

513 TGIF1 shRNA design and electroporation:

514 TGIF1 shRNA design, validation and cloning was performed as previously described (Roly et al.,
515 2020, Major et al., 2019). Four different shRNAs were designed against TGIF1 ORF, ranked for
516 effectiveness (Clarke et al., 2017) and cloned into RCAS(D)-nBFP plasmid. A PCR-based
517 amplification of the shRNA template along with the chicken U6-4 promoter was used (Lambeth
518 et al., 2015) (Table S1). Their ability to knock down TGIF1 expression was assessed *in vitro* in
519 chicken fibroblastic DF-1 cells. Firstly, DF-1 cells were transfected with the plasmids containing
520 BFP-T2A and a non-specific shRNA (firefly sh774) (Roly et al., 2020) or with 4 different putative
521 shRNA designed for TGIF1 knockdown (sh318, sh364, sh416 and sh998), following the
522 Lipofectamine 2000 protocol (Life Technologies). After all cells were BFP positive, they were
523 transfected with the TOL2-GFP-T2A-TGIF1 overexpression plasmid, a transposase expressing
524 plasmid and a TOL2 plasmid expressing mCherry (as a transfection control) following the
525 Lipofectamine 2000 protocol (Life Technologies). 48 hours post transfection, cells were fixed in
526 4% PFA for 15 minutes, stained with DAPI and imaged using a Leica AF600LX microscope. GFP-
527 T2A-TGIF1 intensity was determined on a per cell basis using an established image analysis
528 pipeline (Major et al., 2017). DAPI was used to identify the cell nuclei and mCherry positive cells
529 were gated for further analysis. TGIF1 sh998 showed the stronger TGIF1/GFP inhibition and was
530 cloned into a TOL2 vector expressing nuclear BFP. TOL2-TGIF1sh998-nBFP or TOL2-
531 Fireflysh774-nBFP (non-silencing shRNA) was *in ovo* co-electroporated with a plasmid
532 expressing transposase and TOL2-ACAGS-GFP (electroporation reporter) into the left coelomic
533 epithelium at E2.5. Urogenital systems were collected at E8.5, sexed and immunofluorescence was
534 performed against different gonadal markers.

535 Immunofluorescence:

536 At least three embryos per time point and/or treatment were examined. Tissues were fixed in 4%
537 paraformaldehyde/PBS for 15 minutes at room temperature. Tissues were cryoprotected in PBS
538 plus 30% sucrose, snap frozen in OCT embedding compound, and sectioned at 10 μ m. Some slides
539 were first subjected to antigen retrieval, using an automated system, the Dako PT Link. Slides
540 were firstly baked at 60 °C for 30 minutes. Retrieval was then performed with the Dako Target
541 retrieval solution, a citrate-based (pH 6.0). Slides were then placed in the retrieval machine and
542 retrieved at 98 °C for 30 minutes. All sections were permeabilized in PBS containing 1% Triton
543 X-100, blocked in PBS 2% BSA for 1 hour, and incubated ON at 4 °C with primary antibodies in
544 1% BSA in PBS. Primary antibodies used: goat anti-GFP (Rockland 600-101-215, 1:500), mouse
545 anti-pan-cytokeratin (Novus Bio NBP2-29429, 1:200), rabbit anti-DMRT1 (in house antibody,
546 1:2000), rabbit anti-SOX9 (Millipore antibody AB5535, 1:4000), rabbit anti-AMH (Abexa
547 ABX132175, 1:1000), rabbit anti-aromatase (in house antibody, 1:5000), mouse anti-fibronectin
548 (Serotec 4470–4339, 1:500) and rabbit anti-CVH (in house antibody 1:500). Alexa Fluor
549 secondary antibodies were used (donkey or goat anti-rabbit, mouse or goat 488 or 594; Life
550 technologies). Sections were counterstained with DAPI and mounted in Fluorsave (Milipore). For
551 WISH samples, sections were processed for antigen retrieval (as mentioned above). After the
552 secondary antibody incubation, sections were treated with 0.3% Sudan Black (w/v) in 70% EtOH
553 (v/v) for 10 minutes followed by 8 quick PBS washes. Sections were counterstained with DAPI
554 and mounted.

555 Image quantification:

556 Gonadal, epithelial, medulla and juxtacortical medulla area were manually quantified using Fiji
557 (Schindelin et al., 2012). Epithelial average thickness was calculated by dividing the epithelial area
558 over the length of the epithelium.

559

560 ACKNOWLEDGEMENTS:

561 The authors acknowledge use of the facilities and technical assistance of Monash Histology
562 Platform, Department of Anatomy and Developmental Biology, Monash University. The authors
563 acknowledge the facilities and technical assistance of Monash Micro Imaging.

564 **COMPETING INTERESTS:**

565 The authors declare no competing or financial interests.

566

567 **FUNDING**

568 This research was funded by Australian Research Council (ARC) Discovery Project # 200100709,
569 awarded to C.A.S.

570 **REFERENCES:**

- 571 ANDREWS, J. E., SMITH, C. A. & SINCLAIR, A. H. 1997. Sites of estrogen receptor and aromatase
572 expression in the chicken embryo. *Gen Comp Endocrinol*, 108, 182-90.
- 573 AYERS, K. L., LAMBETH, L. S., DAVIDSON, N. M., SINCLAIR, A. H., OSHLACK, A. & SMITH, C. A. 2015.
574 Identification of candidate gonadal sex differentiation genes in the chicken embryo using RNA-
575 seq. *BMC Genomics*, 16, 704.
- 576 AYERS, K. L., SINCLAIR, A. H. & SMITH, C. A. 2013. The molecular genetics of ovarian differentiation in the
577 avian model. *Sex Dev*, 7, 80-94.
- 578 AYYAR, S., JIANG, J., COLLU, A., WHITE-COOPER, H. & WHITE, R. A. 2003. Drosophila TGIF is essential for
579 developmentally regulated transcription in spermatogenesis. *Development*, 130, 2841-52.
- 580 BANNISTER, S. C., SMITH, C. A., ROESZLER, K. N., DORAN, T. J., SINCLAIR, A. H. & TIZARD, M. L. 2011.
581 Manipulation of estrogen synthesis alters MIR202* expression in embryonic chicken gonads.
582 *Biol Reprod*, 85, 22-30.
- 583 BARRIOS, F., FILIPPONI, D., PELLEGRINI, M., PARONETTO, M. P., DI SIENA, S., GEREMIA, R., ROSSI, P., DE
584 FELICI, M., JANNINI, E. A. & DOLCI, S. 2010. Opposing effects of retinoic acid and FGF9 on
585 Nanos2 expression and meiotic entry of mouse germ cells. *J Cell Sci*, 123, 871-80.
- 586 BERTOLINO, E., REIMUND, B., WILDT-PERINIC, D. & CLERC, R. G. 1995. A novel homeobox protein which
587 recognizes a TGT core and functionally interferes with a retinoid-responsive motif. *J Biol Chem*,
588 270, 31178-88.
- 589 BOWLES, J., FENG, C. W., SPILLER, C., DAVIDSON, T. L., JACKSON, A. & KOOPMAN, P. 2010. FGF9
590 suppresses meiosis and promotes male germ cell fate in mice. *Dev Cell*, 19, 440-9.
- 591 BRENNAN, J. & CAPEL, B. 2004. One tissue, two fates: molecular genetic events that underlie testis
592 versus ovary development. *Nat Rev Genet*, 5, 509-21.
- 593 CAPEL, B. 2017. Vertebrate sex determination: evolutionary plasticity of a fundamental switch. *Nat Rev*
594 *Genet*, 18, 675-689.
- 595 CASTILLO, H. A., CRAVO, R. M., AZAMBUJA, A. P., SIMOES-COSTA, M. S., SURA-TRUEBA, S., GONZALEZ, J.,
596 SLONIMSKY, E., ALMEIDA, K., ABREU, J. G., DE ALMEIDA, M. A., SOBREIRA, T. P., DE OLIVEIRA, S.
597 H., DE OLIVEIRA, P. S., SIGNORE, I. A., COLOMBO, A., CONCHA, M. L., SPENGLER, T. S., BRONNER-
598 FRASER, M., NOBREGA, M., ROSENTHAL, N. & XAVIER-NETO, J. 2010. Insights into the

- 599 organization of dorsal spinal cord pathways from an evolutionarily conserved raldh2 intronic
600 enhancer. *Development*, 137, 507-18.
- 601 CHASSOT, A. A., RANC, F., GREGOIRE, E. P., ROEPERS-GAJADIEN, H. L., TAKETO, M. M., CAMERINO, G., DE
602 ROOIJ, D. G., SCHEDL, A. & CHABOISSIER, M. C. 2008. Activation of beta-catenin signaling by
603 Rspo1 controls differentiation of the mammalian ovary. *Hum Mol Genet*, 17, 1264-77.
- 604 CHEN, M., ZHANG, L., CUI, X., LIN, X., LI, Y., WANG, Y., WANG, Y., QIN, Y., CHEN, D., HAN, C., ZHOU, B.,
605 HUFF, V. & GAO, F. 2017. Wt1 directs the lineage specification of sertoli and granulosa cells by
606 repressing Sf1 expression. *Development*, 144, 44-53.
- 607 CLARKE, B. D., MCCOLL, K. A., WARD, A. C. & DORAN, T. J. 2017. shRNAs targeting either the
608 glycoprotein or polymerase genes inhibit Viral haemorrhagic septicaemia virus replication in
609 zebrafish ZF4 cells. *Antiviral Res*, 141, 124-132.
- 610 CLINTON, M., HAINES, L., BELLOIR, B. & MCBRIDE, D. 2001. Sexing chick embryos: a rapid and simple
611 protocol. *Br Poult Sci*, 42, 134-8.
- 612 COLVIN, J. S., GREEN, R. P., SCHMAHL, J., CAPEL, B. & ORNITZ, D. M. 2001. Male-to-female sex reversal in
613 mice lacking fibroblast growth factor 9. *Cell*, 104, 875-89.
- 614 DEFALCO, T., TAKAHASHI, S. & CAPEL, B. 2011. Two distinct origins for Leydig cell progenitors in the fetal
615 testis. *Dev Biol*, 352, 14-26.
- 616 DINAPOLI, L., BATCHVAROV, J. & CAPEL, B. 2006. FGF9 promotes survival of germ cells in the fetal testis.
617 *Development*, 133, 1519-27.
- 618 ELBRECHT, A. & SMITH, R. G. 1992. Aromatase enzyme activity and sex determination in chickens.
619 *Science*, 255, 467-70.
- 620 ESTERMANN, M. A., WILLIAMS, S., HIRST, C. E., ROLY, Z. Y., SERRALBO, O., ADHIKARI, D., POWELL, D.,
621 MAJOR, A. T. & SMITH, C. A. 2020. Insights into Gonadal Sex Differentiation Provided by Single-
622 Cell Transcriptomics in the Chicken Embryo. *Cell Rep*, 31, 107491.
- 623 FUJIMOTO, Y., TANAKA, S. S., YAMAGUCHI, Y. L., KOBAYASHI, H., KUROKI, S., TACHIBANA, M.,
624 SHINOMURA, M., KANAI, Y., MOROHASHI, K., KAWAKAMI, K. & NISHINAKAMURA, R. 2013.
625 Homeoproteins Six1 and Six4 regulate male sex determination and mouse gonadal
626 development. *Dev Cell*, 26, 416-30.
- 627 GANDHI, S., EZIN, M. & BRONNER, M. E. 2020. Reprogramming Axial Level Identity to Rescue Neural-
628 Crest-Related Congenital Heart Defects. *Dev Cell*, 53, 300-315 e4.
- 629 GASC, J. M. & STUMPF, W. E. 1981. Sexual differentiation of the urogenital tract in the chicken embryo:
630 autoradiographic localization of sex-steroid target cells during development. *J Embryol Exp*
631 *Morphol*, 63, 207-23.
- 632 GONEN, N. & LOVELL-BADGE, R. 2019. The regulation of Sox9 expression in the gonad. *Curr Top Dev Biol*,
633 134, 223-252.
- 634 GONEN, N., QUINN, A., O'NEILL, H. C., KOOPMAN, P. & LOVELL-BADGE, R. 2017. Normal Levels of Sox9
635 Expression in the Developing Mouse Testis Depend on the TES/TESCO Enhancer, but This Does
636 Not Act Alone. *PLoS Genet*, 13, e1006520.
- 637 GONGAL, P. A. & WASKIEWICZ, A. J. 2008. Zebrafish model of holoprosencephaly demonstrates a key
638 role for TGIF in regulating retinoic acid metabolism. *Hum Mol Genet*, 17, 525-38.
- 639 GONZALEZ-MORAN, M. G. 2014. Changes in the cellular localization of estrogen receptor alpha in the
640 growing and regressing ovaries of Gallus domesticus during development. *Biochem Biophys Res*
641 *Commun*, 447, 197-204.
- 642 GUIOLI, S. & LOVELL-BADGE, R. 2007. PITX2 controls asymmetric gonadal development in both sexes of
643 the chick and can rescue the degeneration of the right ovary. *Development*, 134, 4199-208.
- 644 GUIOLI, S., NANDI, S., ZHAO, D., BURGESS-SHANNON, J., LOVELL-BADGE, R. & CLINTON, M. 2014.
645 Gonadal asymmetry and sex determination in birds. *Sex Dev*, 8, 227-42.

- 646 GUIOLI, S., ZHAO, D., NANDI, S., CLINTON, M. & LOVELL-BADGE, R. 2020. Oestrogen in the chick embryo
647 can induce chromosomally male ZZ left gonad epithelial cells to form an ovarian cortex that can
648 support oogenesis. *Development*, 147.
- 649 GUSTIN, S. E., STRINGER, J. M., HOGG, K., SINCLAIR, A. H. & WESTERN, P. S. 2016. FGF9, activin and
650 TGFbeta promote testicular characteristics in an XX gonad organ culture model. *Reproduction*,
651 152, 529-43.
- 652 HACKER, A., CAPEL, B., GOODFELLOW, P. & LOVELL-BADGE, R. 1995. Expression of Sry, the mouse sex
653 determining gene. *Development*, 121, 1603-14.
- 654 HAIDER, M. T., SAITO, H., ZARRER, J., UZHUNNUMPURAM, K., NAGARAJAN, S., KARI, V., HORN-GLANDER,
655 M., WERNER, S., HESSE, E. & TAIPALEENMAKI, H. 2020. Breast cancer bone metastases are
656 attenuated in a Tgif1-deficient bone microenvironment. *Breast Cancer Res*, 22, 34.
- 657 HAMBURGER, V. & HAMILTON, H. L. 1951. A series of normal stages in the development of the chick
658 embryo. *J Morphol*, 88, 49-92.
- 659 HATANO, A., MATSUMOTO, M., HIGASHINAKAGAWA, T. & NAKAYAMA, K. I. 2010. Phosphorylation of
660 the chromodomain changes the binding specificity of Cbx2 for methylated histone H3. *Biochem*
661 *Biophys Res Commun*, 397, 93-9.
- 662 HIRST, C. E., MAJOR, A. T., AYERS, K. L., BROWN, R. J., MARIETTE, M., SACKTON, T. B. & SMITH, C. A.
663 2017a. Sex Reversal and Comparative Data Undermine the W Chromosome and Support Z-linked
664 DMRT1 as the Regulator of Gonadal Sex Differentiation in Birds. *Endocrinology*, 158, 2970-2987.
- 665 HIRST, C. E., SERRALBO, O., AYERS, K. L., ROESZLER, K. N. & SMITH, C. A. 2017b. Genetic Manipulation of
666 the Avian Urogenital System Using In Ovo Electroporation. In: SHENG, G. (ed.) *Avian and*
667 *Reptilian Developmental Biology: Methods and Protocols*. New York, NY: Springer New York.
- 668 HU, S., ZHU, M., WANG, J., LI, L., HE, H., HU, B., HU, J. & XIA, L. 2021. Histomorphology and gene
669 expression profiles during early ovarian folliculogenesis in duck and goose. *Poult Sci*, 100, 1098-
670 1108.
- 671 HU, Y., YU, H., SHAW, G., RENFREE, M. B. & PASK, A. J. 2011. Differential roles of TGIF family genes in
672 mammalian reproduction. *BMC Dev Biol*, 11, 58.
- 673 IOANNIDIS, J., TAYLOR, G., ZHAO, D., LIU, L., IDOKO-AKOH, A., GONG, D., LOVELL-BADGE, R., GUIOLI, S.,
674 MCGREW, M. & CLINTON, M. 2020. Primary sex determination in chickens depends on DMRT1
675 dosage, but gonadal sex does not determine secondary sexual characteristics in adult birds.
676 *bioRxiv*, 2020.09.18.303040.
- 677 IOANNIDIS, J., TAYLOR, G., ZHAO, D., LIU, L., IDOKO-AKOH, A., GONG, D., LOVELL-BADGE, R., GUIOLI, S.,
678 MCGREW, M. J. & CLINTON, M. 2021. Primary sex determination in birds depends on DMRT1
679 dosage, but gonadal sex does not determine adult secondary sex characteristics. *Proc Natl Acad*
680 *Sci U S A*, 118.
- 681 ISHIMARU, Y., KOMATSU, T., KASAHARA, M., KATOH-FUKUI, Y., OGAWA, H., TOYAMA, Y., MAEKAWA, M.,
682 TOSHIMORI, K., CHANDRARATNA, R. A., MOROHASHI, K. & YOSHIOKA, H. 2008. Mechanism of
683 asymmetric ovarian development in chick embryos. *Development*, 135, 677-85.
- 684 JOHNSON, A. L. & WOODS, D. C. 2009. Dynamics of avian ovarian follicle development: cellular
685 mechanisms of granulosa cell differentiation. *Gen Comp Endocrinol*, 163, 12-7.
- 686 JORDAN, B. K., SHEN, J. H., OLASO, R., INGRAHAM, H. A. & VILAIN, E. 2003. Wnt4 overexpression
687 disrupts normal testicular vasculature and inhibits testosterone synthesis by repressing
688 steroidogenic factor 1/beta-catenin synergy. *Proc Natl Acad Sci U S A*, 100, 10866-71.
- 689 KARL, J. & CAPEL, B. 1998. Sertoli cells of the mouse testis originate from the coelomic epithelium. *Dev*
690 *Biol*, 203, 323-33.
- 691 KASHIMADA, K. & KOOPMAN, P. 2010. Sry: the master switch in mammalian sex determination.
692 *Development*, 137, 3921-30.

- 693 KASHIMADA, K., PELOSI, E., CHEN, H., SCHLESSINGER, D., WILHELM, D. & KOOPMAN, P. 2011. FOXL2 and
694 BMP2 act cooperatively to regulate follistatin gene expression during ovarian development.
695 *Endocrinology*, 152, 272-80.
- 696 KENT, J., WHEATLEY, S. C., ANDREWS, J. E., SINCLAIR, A. H. & KOOPMAN, P. 1996. A male-specific role for
697 SOX9 in vertebrate sex determination. *Development*, 122, 2813-22.
- 698 KIM, Y., BINGHAM, N., SEKIDO, R., PARKER, K. L., LOVELL-BADGE, R. & CAPEL, B. 2007. Fibroblast growth
699 factor receptor 2 regulates proliferation and Sertoli differentiation during male sex
700 determination. *Proc Natl Acad Sci U S A*, 104, 16558-63.
- 701 KIM, Y., KOBAYASHI, A., SEKIDO, R., DINAPOLI, L., BRENNAN, J., CHABOISSIER, M. C., POULAT, F.,
702 BEHRINGER, R. R., LOVELL-BADGE, R. & CAPEL, B. 2006. Fgf9 and Wnt4 act as antagonistic signals
703 to regulate mammalian sex determination. *PLoS Biol*, 4, e187.
- 704 KOOPMAN, P., GUBBAY, J., VIVIAN, N., GOODFELLOW, P. & LOVELL-BADGE, R. 1991. Male development
705 of chromosomally female mice transgenic for Sry. *Nature*, 351, 117-21.
- 706 KUSAKA, M., KATOH-FUKUI, Y., OGAWA, H., MIYABAYASHI, K., BABA, T., SHIMA, Y., SUGIYAMA, N.,
707 SUGIMOTO, Y., OKUNO, Y., KODAMA, R., IIZUKA-KOGO, A., SENDA, T., SASAOKA, T., KITAMURA,
708 K., AIZAWA, S. & MOROHASHI, K. 2010. Abnormal epithelial cell polarity and ectopic epidermal
709 growth factor receptor (EGFR) expression induced in Emx2 KO embryonic gonads.
710 *Endocrinology*, 151, 5893-904.
- 711 LAMBETH, L. S., AYERS, K., CUTTING, A. D., DORAN, T. J., SINCLAIR, A. H. & SMITH, C. A. 2015. Anti-
712 Mullerian Hormone Is Required for Chicken Embryonic Urogenital System Growth but Not
713 Sexual Differentiation. *Biol Reprod*, 93, 138.
- 714 LAMBETH, L. S., RAYMOND, C. S., ROESZLER, K. N., KUROIWA, A., NAKATA, T., ZARKOWER, D. & SMITH,
715 C. A. 2014. Over-expression of DMRT1 induces the male pathway in embryonic chicken gonads.
716 *Dev Biol*, 389, 160-72.
- 717 LAU, Y. F. & LI, Y. 2009. The human and mouse sex-determining SRY genes repress the Rspol/beta-
718 catenin signaling. *J Genet Genomics*, 36, 193-202.
- 719 LAVERY, R., CHASSOT, A. A., PAUPER, E., GREGOIRE, E. P., KLOPFENSTEIN, M., DE ROOIJ, D. G., MARK, M.,
720 SCHEDL, A., GHYSELINCK, N. B. & CHABOISSIER, M. C. 2012. Testicular differentiation occurs in
721 absence of R-spondin1 and Sox9 in mouse sex reversals. *PLoS Genet*, 8, e1003170.
- 722 LEE, B. K., SHEN, W., LEE, J., RHEE, C., CHUNG, H., KIM, K. Y., PARK, I. H. & KIM, J. 2015. Tgif1
723 Counterbalances the Activity of Core Pluripotency Factors in Mouse Embryonic Stem Cells. *Cell*
724 *Rep*, 13, 52-60.
- 725 LI, J., ZHAO, D., GUO, C., LI, J., MI, Y. & ZHANG, C. 2016. Involvement of Notch signaling in early chick
726 ovarian follicle development. *Cell Biol Int*, 40, 65-73.
- 727 LI, Y., ZHANG, L., HU, Y., CHEN, M., HAN, F., QIN, Y., CHEN, M., CUI, X., DUO, S., TANG, F. & GAO, F. 2017.
728 beta-Catenin directs the transformation of testis Sertoli cells to ovarian granulosa-like cells by
729 inducing Foxl2 expression. *J Biol Chem*, 292, 17577-17586.
- 730 LI, Y., ZHENG, M. & LAU, Y. F. 2014. The sex-determining factors SRY and SOX9 regulate similar target
731 genes and promote testis cord formation during testicular differentiation. *Cell Rep*, 8, 723-33.
- 732 LIN, Y. T., BARSKE, L., DEFALCO, T. & CAPEL, B. 2017. Numb regulates somatic cell lineage commitment
733 during early gonadogenesis in mice. *Development*, 144, 1607-1618.
- 734 LIN, Y. T. & CAPEL, B. 2015. Cell fate commitment during mammalian sex determination. *Curr Opin Genet*
735 *Dev*, 32, 144-52.
- 736 LIU, C., PENG, J., MATZUK, M. M. & YAO, H. H. 2015. Lineage specification of ovarian theca cells requires
737 multicellular interactions via oocyte and granulosa cells. *Nat Commun*, 6, 6934.
- 738 LIU, X., ZHANG, H., GAO, L., YIN, Y., PAN, X., LI, Z., LI, N., LI, H. & YU, Z. 2014. Negative interplay of
739 retinoic acid and TGF-beta signaling mediated by TG-interacting factor to modulate mouse

- 740 embryonic palate mesenchymal-cell proliferation. *Birth Defects Res B Dev Reprod Toxicol*, 101,
741 403-9.
- 742 LORDA-DIEZ, C. I., MONTERO, J. A., MARTINEZ-CUE, C., GARCIA-PORRERO, J. A. & HURLE, J. M. 2009.
743 Transforming growth factors beta coordinate cartilage and tendon differentiation in the
744 developing limb mesenchyme. *J Biol Chem*, 284, 29988-96.
- 745 MAATOUK, D. M., DINAPOLI, L., ALVERS, A., PARKER, K. L., TAKETO, M. M. & CAPEL, B. 2008. Stabilization
746 of beta-catenin in XY gonads causes male-to-female sex-reversal. *Hum Mol Genet*, 17, 2949-55.
- 747 MAJOR, A. T., AYERS, K., CHUE, J., ROESZLER, K. & SMITH, C. 2019. FOXL2 antagonises the male
748 developmental pathway in embryonic chicken gonads. *J Endocrinol*.
- 749 MAJOR, A. T., MIYAMOTO, Y., LO, C. Y., JANS, D. A. & LOVELAND, K. L. 2017. Development of a pipeline
750 for automated, high-throughput analysis of paraspeckle proteins reveals specific roles for
751 importin alpha proteins. *Sci Rep*, 7, 43323.
- 752 MELHUIH, T. A. & WOTTON, D. 2000. The interaction of the carboxyl terminus-binding protein with the
753 Smad corepressor TGIF is disrupted by a holoprosencephaly mutation in TGIF. *J Biol Chem*, 275,
754 39762-6.
- 755 MENDEZ, C., ALCANTARA, L., ESCALONA, R., LOPEZ-CASILLAS, F. & PEDERNEIRA, E. 2006. Transforming
756 growth factor beta inhibits proliferation of somatic cells without influencing germ cell number in
757 the chicken embryonic ovary. *Cell Tissue Res*, 325, 143-9.
- 758 MUNGER, S. C. & CAPEL, B. 2012. Sex and the circuitry: progress toward a systems-level understanding
759 of vertebrate sex determination. *Wiley Interdiscip Rev Syst Biol Med*, 4, 401-12.
- 760 NEF, S., STEVANT, I. & GREENFIELD, A. 2019. Characterizing the bipotential mammalian gonad. *Curr Top*
761 *Dev Biol*, 134, 167-194.
- 762 NICOL, B. & YAO, H. H. 2014. Building an ovary: insights into establishment of somatic cell lineages in the
763 mouse. *Sex Dev*, 8, 243-51.
- 764 NIU, W. & SPRADLING, A. C. 2020. Two distinct pathways of pregranulosa cell differentiation support
765 follicle formation in the mouse ovary. *Proc Natl Acad Sci U S A*, 117, 20015-20026.
- 766 OMOTEHARA, T., MINAMI, K., MANTANI, Y., UMEMURA, Y., NISHIDA, M., HIRANO, T., YOSHIOKA, H.,
767 KITAGAWA, H., YOKOYAMA, T. & HOSHI, N. 2017. Contribution of the coelomic epithelial cells
768 specific to the left testis in the chicken embryo. *Dev Dyn*, 246, 148-156.
- 769 PARMA, P., RADI, O., VIDAL, V., CHABOISSIER, M. C., DELLAMBRA, E., VALENTINI, S., GUERRA, L., SCHEDL,
770 A. & CAMERINO, G. 2006. R-spondin1 is essential in sex determination, skin differentiation and
771 malignancy. *Nat Genet*, 38, 1304-9.
- 772 PFAFFL, M. W. 2001. A new mathematical model for relative quantification in real-time RT-PCR. *Nucleic*
773 *Acids Res*, 29, e45.
- 774 PIEAU, C. & DORIZZI, M. 2004. Oestrogens and temperature-dependent sex determination in reptiles: all
775 is in the gonads. *J Endocrinol*, 181, 367-77.
- 776 POWERS, S. E., TANIGUCHI, K., YEN, W., MELHUIH, T. A., SHEN, J., WALSH, C. A., SUTHERLAND, A. E. &
777 WOTTON, D. 2010. Tgif1 and Tgif2 regulate Nodal signaling and are required for gastrulation.
778 *Development*, 137, 249-59.
- 779 QIN, Y. & BISHOP, C. E. 2005. Sox9 is sufficient for functional testis development producing fertile male
780 mice in the absence of Sry. *Hum Mol Genet*, 14, 1221-9.
- 781 RODRIGUEZ-LEON, J., RODRIGUEZ ESTEBAN, C., MARTI, M., SANTIAGO-JOSEFAT, B., DUBOVA, I.,
782 RUBIRALTA, X. & IZPISUA BELMONTE, J. C. 2008. Pitx2 regulates gonad morphogenesis. *Proc Natl*
783 *Acad Sci U S A*, 105, 11242-7.
- 784 ROLY, Z. Y., MAJOR, A. T., FULCHER, A., ESTERMANN, M. A., HIRST, C. E. & SMITH, C. A. 2020. Adhesion
785 G-protein-coupled receptor, GPR56, is required for Mullerian duct development in the chick. *J*
786 *Endocrinol*, 244, 395-413.

- 787 ROTGERS, E., JORGENSEN, A. & YAO, H. H. 2018. At the Crossroads of Fate-Somatic Cell Lineage
788 Specification in the Fetal Gonad. *Endocr Rev*, 39, 739-759.
- 789 SATO, Y., KASAI, T., NAKAGAWA, S., TANABE, K., WATANABE, T., KAWAKAMI, K. & TAKAHASHI, Y. 2007.
790 Stable integration and conditional expression of electroporated transgenes in chicken embryos.
791 *Dev Biol*, 305, 616-24.
- 792 SCHEIB, D. 1983. Effects and role of estrogens in avian gonadal differentiation. *Differentiation*.
793 1983/01/01 ed.
- 794 SCHINDELIN, J., ARGANDA-CARRERAS, I., FRISE, E., KAYNIG, V., LONGAIR, M., PIETZSCH, T., PREIBISCH, S.,
795 RUEDEN, C., SAALFELD, S., SCHMID, B., TINEVEZ, J. Y., WHITE, D. J., HARTENSTEIN, V., ELICEIRI,
796 K., TOMANCAK, P. & CARDONA, A. 2012. Fiji: an open-source platform for biological-image
797 analysis. *Nat Methods*, 9, 676-82.
- 798 SCHMAHL, J., KIM, Y., COLVIN, J. S., ORNITZ, D. M. & CAPEL, B. 2004. Fgf9 induces proliferation and
799 nuclear localization of FGFR2 in Sertoli precursors during male sex determination. *Development*,
800 131, 3627-36.
- 801 SCHMID, M., SMITH, J., BURT, D. W., AKEN, B. L., ANTIN, P. B., ARCHIBALD, A. L., ASHWELL, C.,
802 BLACKSHEAR, P. J., BOSCHIERO, C., BROWN, C. T., BURGESS, S. C., CHENG, H. H., CHOW, W.,
803 COBLE, D. J., COOKSEY, A., CROOIJMANS, R. P., DAMAS, J., DAVIS, R. V., DE KONING, D. J.,
804 DELANY, M. E., DERRIEN, T., DESTA, T. T., DUNN, I. C., DUNN, M., ELLEGREN, H., EORY, L., ERB, I.,
805 FARRE, M., FASOLD, M., FLEMING, D., FLICEK, P., FOWLER, K. E., FRESARD, L., FROMAN, D. P.,
806 GARCEAU, V., GARDNER, P. P., GHEYAS, A. A., GRIFFIN, D. K., GROENEN, M. A., HAAF, T.,
807 HANOTTE, O., HART, A., HASLER, J., HEDGES, S. B., HERTEL, J., HOWE, K., HUBBARD, A., HUME, D.
808 A., KAISER, P., KEDRA, D., KEMP, S. J., KLOPP, C., KNIEL, K. E., KUO, R., LAGARRIGUE, S., LAMONT,
809 S. J., LARKIN, D. M., LAWAL, R. A., MARKLAND, S. M., MCCARTHY, F., MCCORMACK, H. A.,
810 MCPHERSON, M. C., MOTEGI, A., MULJO, S. A., MUNSTERBERG, A., NAG, R., NANDA, I.,
811 NEUBERGER, M., NITSCHKE, A., NOTREDAME, C., NOYES, H., O'CONNOR, R., O'HARE, E. A., OLER,
812 A. J., OMMEH, S. C., PAIS, H., PERSIA, M., PITEL, F., PREEYANON, L., PRIETO BARJA, P.,
813 PRITCHETT, E. M., RHOADS, D. D., ROBINSON, C. M., ROMANOV, M. N., ROTHSCHILD, M., ROUX,
814 P. F., SCHMIDT, C. J., SCHNEIDER, A. S., SCHWARTZ, M. G., SEARLE, S. M., SKINNER, M. A., SMITH,
815 C. A., STADLER, P. F., STEEVES, T. E., STEINLEIN, C., SUN, L., TAKATA, M., ULITSKY, I., WANG, Q.,
816 WANG, Y., et al. 2015. Third Report on Chicken Genes and Chromosomes 2015. *Cytogenet*
817 *Genome Res*, 145, 78-179.
- 818 SEKIDO, R., BAR, I., NARVAEZ, V., PENNY, G. & LOVELL-BADGE, R. 2004. SOX9 is up-regulated by the
819 transient expression of SRY specifically in Sertoli cell precursors. *Dev Biol*, 274, 271-9.
- 820 SEKIDO, R. & LOVELL-BADGE, R. 2007. Mechanisms of gonadal morphogenesis are not conserved
821 between chick and mouse. *Dev Biol*, 302, 132-42.
- 822 SEKIDO, R. & LOVELL-BADGE, R. 2008. Sex determination involves synergistic action of SRY and SF1 on a
823 specific Sox9 enhancer. *Nature*, 453, 930-4.
- 824 SHEN, J. & WALSH, C. A. 2005. Targeted disruption of Tgif, the mouse ortholog of a human
825 holoprosencephaly gene, does not result in holoprosencephaly in mice. *Mol Cell Biol*, 25, 3639-
826 47.
- 827 SINCLAIR, A. H., BERTA, P., PALMER, M. S., HAWKINS, J. R., GRIFFITHS, B. L., SMITH, M. J., FOSTER, J. W.,
828 FRISCHAUF, A. M., LOVELL-BADGE, R. & GOODFELLOW, P. N. 1990. A gene from the human sex-
829 determining region encodes a protein with homology to a conserved DNA-binding motif. *Nature*,
830 346, 240-4.
- 831 SMITH, C. A., KATZ, M. & SINCLAIR, A. H. 2003. DMRT1 is upregulated in the gonads during female-to-
832 male sex reversal in ZW chicken embryos. *Biol Reprod*, 68, 560-70.
- 833 SMITH, C. A., ROESZLER, K. N., BOWLES, J., KOOPMAN, P. & SINCLAIR, A. H. 2008. Onset of meiosis in the
834 chicken embryo; evidence of a role for retinoic acid. *BMC Dev Biol*, 8, 85.

- 835 SMITH, C. A., ROESZLER, K. N., OHNESORG, T., CUMMINS, D. M., FARLIE, P. G., DORAN, T. J. & SINCLAIR,
836 A. H. 2009. The avian Z-linked gene DMRT1 is required for male sex determination in the
837 chicken. *Nature*, 461, 267-71.
- 838 SMITH, C. A. & SINCLAIR, A. H. 2004. Sex determination: insights from the chicken. *Bioessays*, 26, 120-
839 32.
- 840 SPILLER, C., KOOPMAN, P. & BOWLES, J. 2017. Sex Determination in the Mammalian Germline. *Annu Rev*
841 *Genet*, 51, 265-285.
- 842 STEVANT, I., KUHNE, F., GREENFIELD, A., CHABOISSIER, M. C., DERMITZAKIS, E. T. & NEF, S. 2019.
843 Dissecting Cell Lineage Specification and Sex Fate Determination in Gonadal Somatic Cells Using
844 Single-Cell Transcriptomics. *Cell Rep*, 26, 3272-3283 e3.
- 845 STEVANT, I. & NEF, S. 2019. Genetic Control of Gonadal Sex Determination and Development. *Trends*
846 *Genet*, 35, 346-358.
- 847 STEVANT, I., NEIRIJNCK, Y., BOREL, C., ESCOFFIER, J., SMITH, L. B., ANTONARAKIS, S. E., DERMITZAKIS, E.
848 T. & NEF, S. 2018. Deciphering Cell Lineage Specification during Male Sex Determination with
849 Single-Cell RNA Sequencing. *Cell Rep*, 22, 1589-1599.
- 850 SUN, W., CAI, H., ZHANG, G., ZHANG, H., BAO, H., WANG, L., YE, J., QIAN, G. & GE, C. 2017. Dmrt1 is
851 required for primary male sexual differentiation in Chinese soft-shelled turtle *Pelodiscus*
852 *sinensis*. *Sci Rep*, 7, 4433.
- 853 SVINGEN, T. & KOOPMAN, P. 2013. Building the mammalian testis: origins, differentiation, and assembly
854 of the component cell populations. *Genes Dev*, 27, 2409-26.
- 855 TOMIZUKA, K., HORIKOSHI, K., KITADA, R., SUGAWARA, Y., IBA, Y., KOJIMA, A., YOSHITOME, A.,
856 YAMAWAKI, K., AMAGAI, M., INOUE, A., OSHIMA, T. & KAKITANI, M. 2008. R-spondin1 plays an
857 essential role in ovarian development through positively regulating Wnt-4 signaling. *Hum Mol*
858 *Genet*, 17, 1278-91.
- 859 UKESHIMA, A. 1996. Germ cell death in the degenerating right ovary of the chick embryo. *Zoolog Sci*, 13,
860 559-63.
- 861 VAILLANT, S., DORIZZI, M., PIEAU, C. & RICHARD-MERCIER, N. 2001a. Sex reversal and aromatase in
862 chicken. *J Exp Zool*, 290, 727-40.
- 863 VAILLANT, S., MAGRE, S., DORIZZI, M., PIEAU, C. & RICHARD-MERCIER, N. 2001b. Expression of AMH,
864 SF1, and SOX9 in gonads of genetic female chickens during sex reversal induced by an aromatase
865 inhibitor. *Dev Dyn*, 222, 228-37.
- 866 VIDAL, V. P., CHABOISSIER, M. C., DE ROOIJ, D. G. & SCHEDL, A. 2001. Sox9 induces testis development in
867 XX transgenic mice. *Nat Genet*, 28, 216-7.
- 868 WANG, J. L., QI, Z., LI, Y. H., ZHAO, H. M., CHEN, Y. G. & FU, W. 2017. TGFbeta induced factor homeobox
869 1 promotes colorectal cancer development through activating Wnt/beta-catenin signaling.
870 *Oncotarget*, 8, 70214-70225.
- 871 WARTENBERG, H., LENZ, E. & SCHWEIKERT, H. U. 1992. Sexual differentiation and the germ cell in sex
872 reversed gonads after aromatase inhibition in the chicken embryo. *Andrologia*, 24, 1-6.
- 873 WEAR, H. M., ERIKSSON, A., YAO, H. H. & WATANABE, K. H. 2017. Cell-based computational model of
874 early ovarian development in mice. *Biol Reprod*, 97, 365-377.
- 875 WOTTON, D., KNOEPFLER, P. S., LAHERTY, C. D., EISENMAN, R. N. & MASSAGUE, J. 2001. The Smad
876 transcriptional corepressor TGIF recruits mSin3. *Cell Growth Differ*, 12, 457-63.
- 877 WOTTON, D., LO, R. S., LEE, S. & MASSAGUE, J. 1999a. A Smad transcriptional corepressor. *Cell*, 97, 29-
878 39.
- 879 WOTTON, D., LO, R. S., SWABY, L. A. & MASSAGUE, J. 1999b. Multiple modes of repression by the Smad
880 transcriptional corepressor TGIF. *J Biol Chem*, 274, 37105-10.

- 881 WU, Q., KANATA, K., SABA, R., DENG, C. X., HAMADA, H. & SAGA, Y. 2013. Nodal/activin signaling
882 promotes male germ cell fate and suppresses female programming in somatic cells.
883 *Development*, 140, 291-300.
- 884 XIANG, G., YI, Y., WEIWEI, H. & WEIMING, W. 2015. TGIF1 promoted the growth and migration of cancer
885 cells in nonsmall cell lung cancer. *Tumour Biol*, 36, 9303-10.
- 886 YAO, H. H., WHORISKEY, W. & CAPEL, B. 2002. Desert Hedgehog/Patched 1 signaling specifies fetal
887 Leydig cell fate in testis organogenesis. *Genes Dev*, 16, 1433-40.
- 888 ZHANG, L., CHEN, M., WEN, Q., LI, Y., WANG, Y., WANG, Y., QIN, Y., CUI, X., YANG, L., HUFF, V. & GAO, F.
889 2015a. Reprogramming of Sertoli cells to fetal-like Leydig cells by Wt1 ablation. *Proc Natl Acad*
890 *Sci U S A*, 112, 4003-8.
- 891 ZHANG, M. Z., FERRIGNO, O., WANG, Z., OHNISHI, M., PRUNIER, C., LEVY, L., RAZZAQUE, M., HORNE, W.
892 C., ROMERO, D., TZIVION, G., COLLAND, F., BARON, R. & ATFI, A. 2015b. TGIF governs a feed-
893 forward network that empowers Wnt signaling to drive mammary tumorigenesis. *Cancer Cell*,
894 27, 547-60.
- 895
- 896

897 **FIGURE LEGENDS:**

898 **Fig. 1. *TGIF1* expression profile in chicken gonads.** (A) *TGIF1* gonadal RNA-seq mRNA
899 expression levels in count per million (CPM) at blastoderm stage, before (E4.5) and on the onset
900 (E6) of sex determination. # = false discovery rate (FDR) <0.001. (B) *TGIF1* gonadal mRNA was
901 quantified by qRT-PCR. Expression level is relative to β -actin and normalized to E4.5 female.
902 (Bars represent Mean \pm SEM, n=6. * = adjusted p value <0.05. Multiple t-test and Holm-Sidak
903 posttest. (C) *TGIF1* time course mRNA expression in embryonic chicken gonads, as assessed by
904 whole mount *in situ* hybridization. (D) Sections of the *TGIF1* whole mounts *in situ* hybridizations.
905 Arrows indicate the cortex (C), epithelium (E), medulla (M) and seminiferous cords (SC). Dashed
906 black lines indicate the cortical-medulla limit.

907

908 **Fig. 2. *TGIF1* expression colocalizes with key ovarian cells.** *TGIF1* whole mount *in situ*
909 hybridization was performed in E6.5 and E8.5 female urogenital systems. 10 μ m sections were
910 processed for immunofluorescence against Cytokeratin (cortical cells marker) and Aromatase (pre-
911 granulosa cells marker). *TGIF1* expression colocalize with both female markers in left ovaries.
912 Arrows indicate the interstitial (I), cortical (C), medullary cords (MC), epithelial (E) and
913 juxtacortical medulla (JCM) cells.

914

915 **Fig. 3. Estrogens induce *TGIF1* expression in ZZ gonads.** *TGIF1* whole mount *in situ*
916 hybridization was performed in E9.5 male and female urogenital systems treated *in ovo* with 17 β -
917 estradiol (E2) or vehicle (Control). Tissues were sectioned and immunofluorescence for aromatase
918 (pre-granulosa marker) or AMH (Sertoli cell marker) and Cytokeratin (cortical marker) were
919 performed to evaluate the efficacy of the sex reversal.

920

921 **Fig. 4. Estrogen synthesis inhibition by fadrozole results in downregulation of *TGIF1* in ZW**
922 **gonads.** (A) *TGIF1* whole mount *in situ* hybridization was performed in E9.5 male and female
923 urogenital systems treated *in ovo* with the aromatase inhibitor fadrozole (AI) or vehicle (Control).
924 Tissues were sectioned and immunofluorescence for aromatase (pre-granulosa marker) or AMH
925 (Sertoli cell marker) and Cytokeratin (cortical marker) were performed to evaluate the efficacy of
926 the sex reversal. (B) *TGIF1* qRT-PCR was performed in gonadal samples of E9.5 embryos treated

927 with the aromatase inhibitor (AI) or vehicle (Control). Expression level is relative to β -actin and
928 normalized to male PBS. Bars represent Mean \pm SEM, n=6. ** = adjusted p value <0.01. Multiple
929 t-test and Holm-Sidak posttest.

930

931 **Fig. 5. TGIF1 overexpression results in epithelial thickening.** TOL2 TGIF1 overexpression
932 (TGIF1 OE) or control (GFP Control) plasmids were electroporated in male left E2.5 coelomic
933 epithelium. Gonads were examined at E8.5. (A) Immunofluorescence against cytokeratin
934 (epithelial/cortical marker) were performed in transverse sections. Dashed box indicates the
935 magnified area. Dotted line delineates the gonadal epithelium. White arrow indicates the
936 epithelium (E), white arrowhead indicates EMT derived interstitial cell and M indicates medulla.
937 (B) Quantification of the percentage of epithelial area, related to the total gonadal area in male
938 gonads. (C) Quantification of the average epithelium thickness (in μ m) in control or TGIF1
939 overexpressing male gonads. Bars represent Mean \pm SEM, n \geq 6. Unpaired two-tailed t-test. * = p
940 value <0.05.

941

942 **Fig. 6 TGIF1 overexpression results in gonadal feminization.** TOL2 TGIF1 overexpression
943 (TGIF1 OE) or control (GFP Control) plasmids were electroporated in male left E2.5 coelomic
944 epithelium. Gonads were examined at E8.5. Immunofluorescence against (A) fibronectin
945 (interstitial cell marker) and (B) AMH (Sertoli cell marker) were performed in transverse sections.
946 Dashed box indicates the magnified area. Dotted line delineates the gonadal epithelium. Arrows
947 indicate the juxtacortical medulla (JCM). (C) Quantification of the percentage of juxtacortical
948 medulla area, related to the total medullar area. Bars represent Mean \pm SEM, n \geq 7. Unpaired two-
949 tailed t-test. *** = p value <0.001.

950

951 **Fig. 7. TGIF1 RCAS overexpression mimics the results from TGIF1 TOL2 overexpression.**
952 RCAS(A) TGIF1 overexpression (TGIF1 OE) or control (GFP OE) plasmids were electroporated
953 in male left E2.5 coelomic epithelium. Male gonads were examined at E8.5 and
954 immunofluorescence against cytokeratin (epithelial/cortical marker) was performed in
955 longitudinal sections. Dashed box indicates the magnified area. Dotted line delineates the gonadal
956 epithelium. White arrows indicate the gonadal epithelium (E). M indicates the medulla.

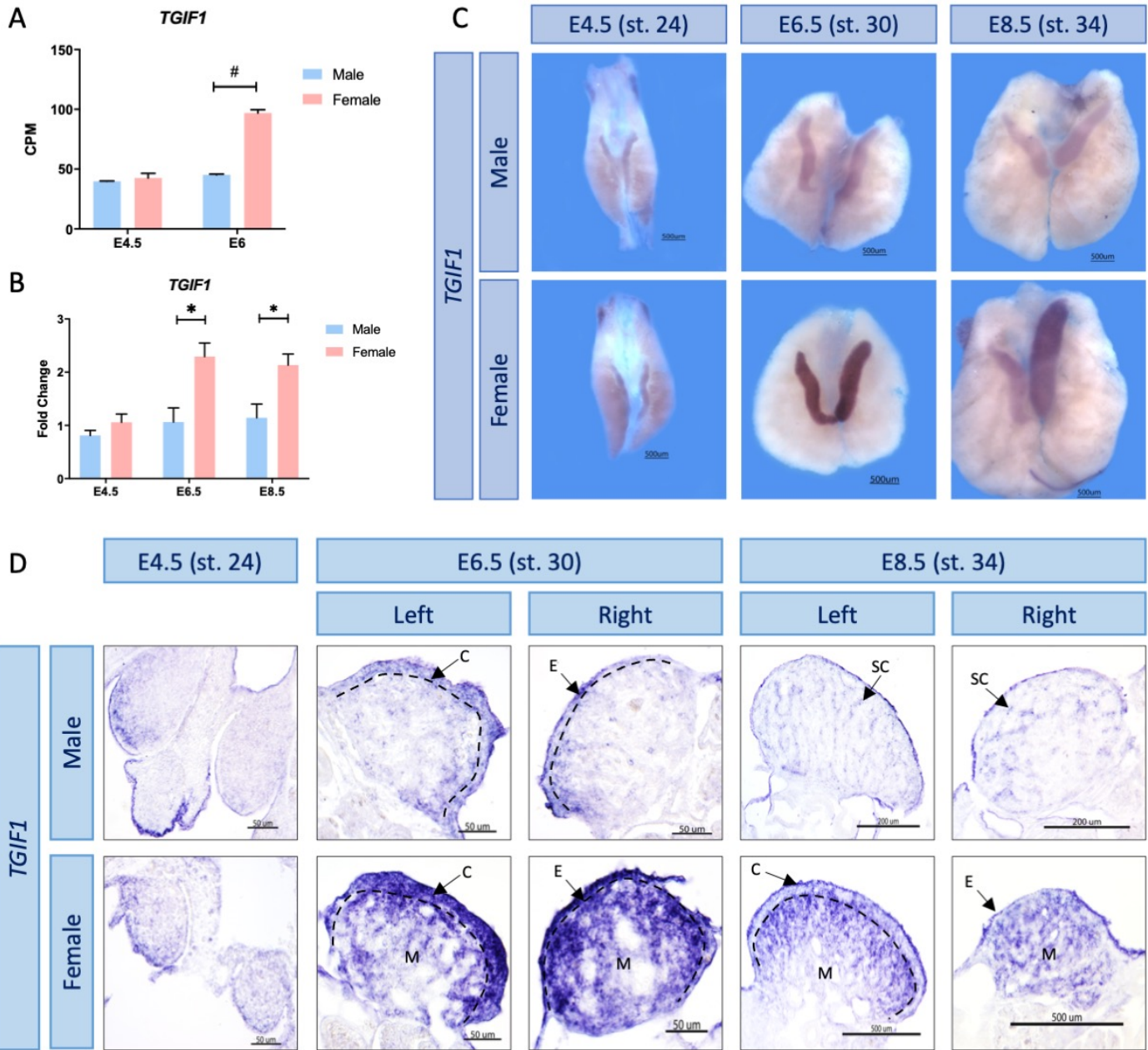
957 **Fig. 8. TGIF1 sh998 showed the higher repression of TGIF1 in vitro.** Chicken DF-1 cells were
958 transfected with a self-replicative viral plasmid containing BFP-T2A and a non-specific shRNA
959 (NS shRNA) or with 4 different putative shRNA designed for TGIF1 knockdown (sh318, sh364,
960 sh416 or sh998). After all cells were BFP positive, they were transfected with the overexpression
961 TOL2-GFP-T2A-TGIF1 plasmid and a plasmid expressing mCherry (as a transfection control).
962 After 48 hours cells were fixed and analyzed under the microscope. (A) Representative
963 fluorescence images of the outcomes. (B) Imaris analysis of the GFP-T2A-TGIF intensity in
964 mCherry positive (transfected) cells. Box plots show each sample's median, interquartile ranges
965 (IQR) and the whiskers extend to the highest/lowest value within 1.5 x IQR. Each dot represents
966 an individual cell. t-test was performed using NS shRNA as a control condition. Dunnett's multiple
967 comparisons test was used as posttest. *****, $p < 0.0001$.

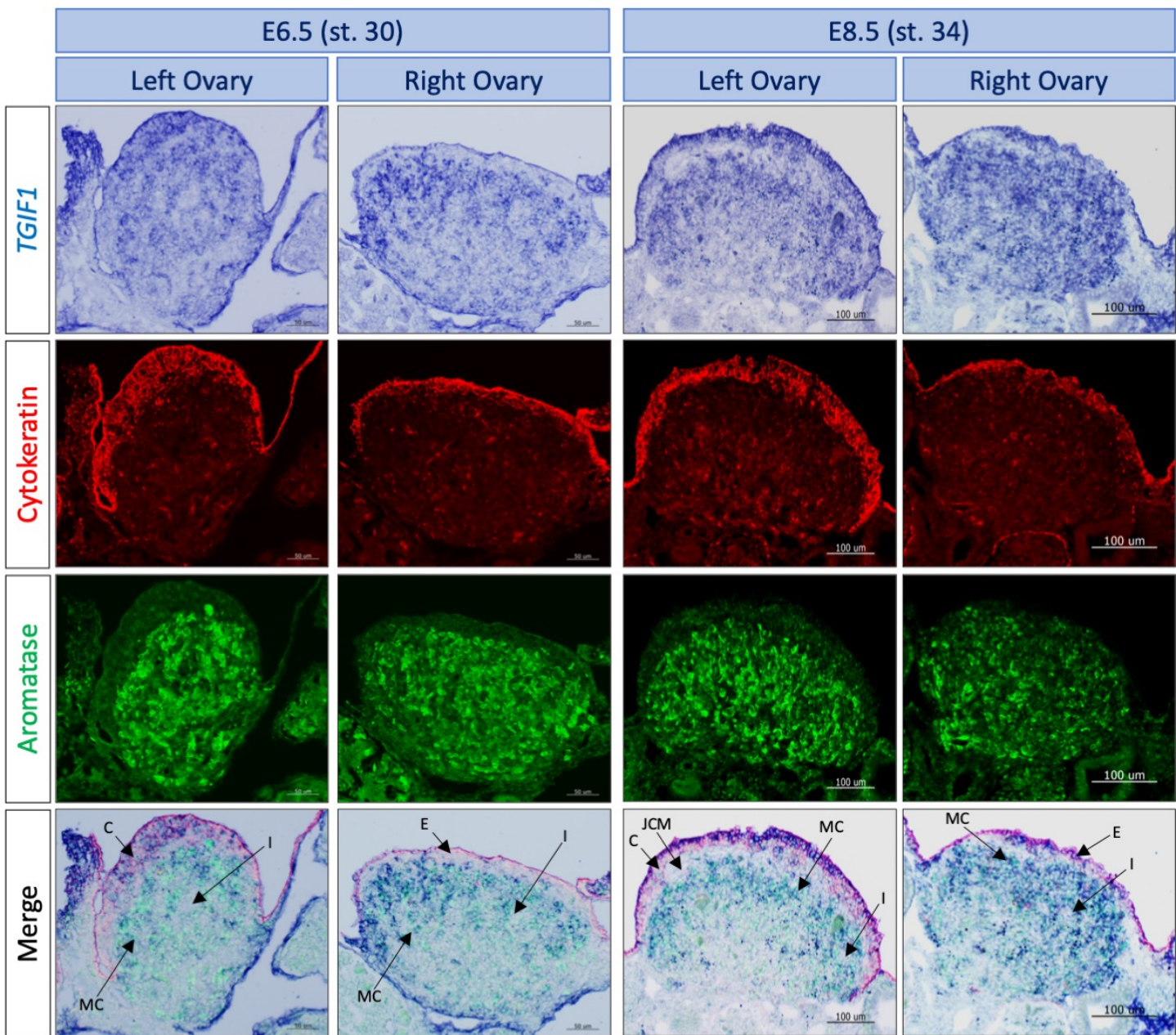
968

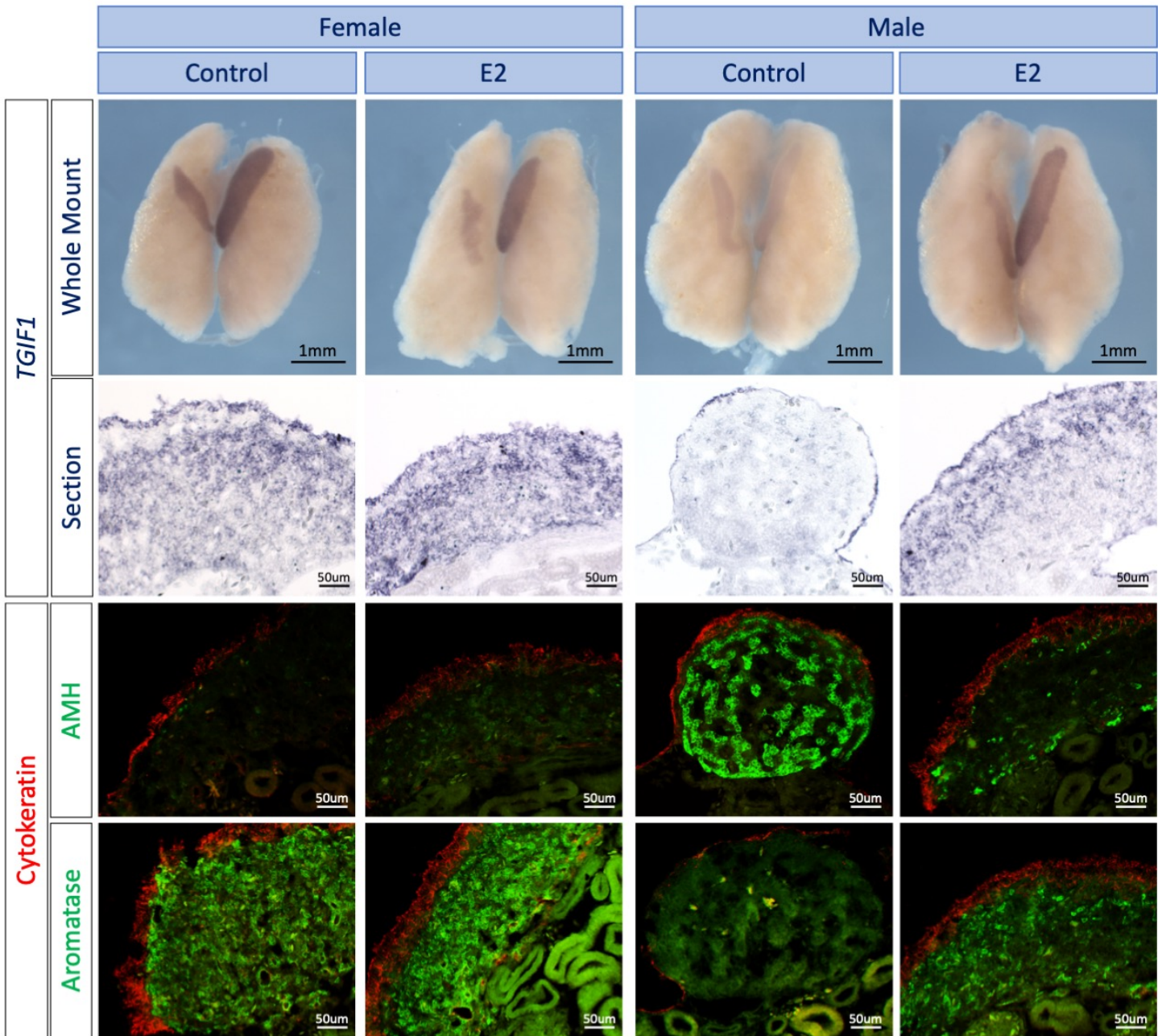
969 **Fig. 9. TGIF1 Knock down ablates cortical and juxtacortical medulla formation in female**
970 **gonads.** TOL2 TGIF1 knock down (TGIF1 sh998) or non-silencing control (NS shRNA) plasmids
971 were co-electroporated with a GFP expressing plasmid (reporter) in female left E2.5 coelomic
972 epithelium. Gonads were examined at E8.5. Immunofluorescence against (A) aromatase (pre-
973 granulosa marker), (B) cytokeratin (epithelial/cortical marker), (C) fibronectin (interstitial cell
974 marker) and (D) CVH (germ cell marker) were performed in transverse sections. Dashed line
975 delineates the gonadal epithelium. Arrows indicate the cortex (C) or the juxtacortical medulla
976 (JCM). M indicates the medulla.

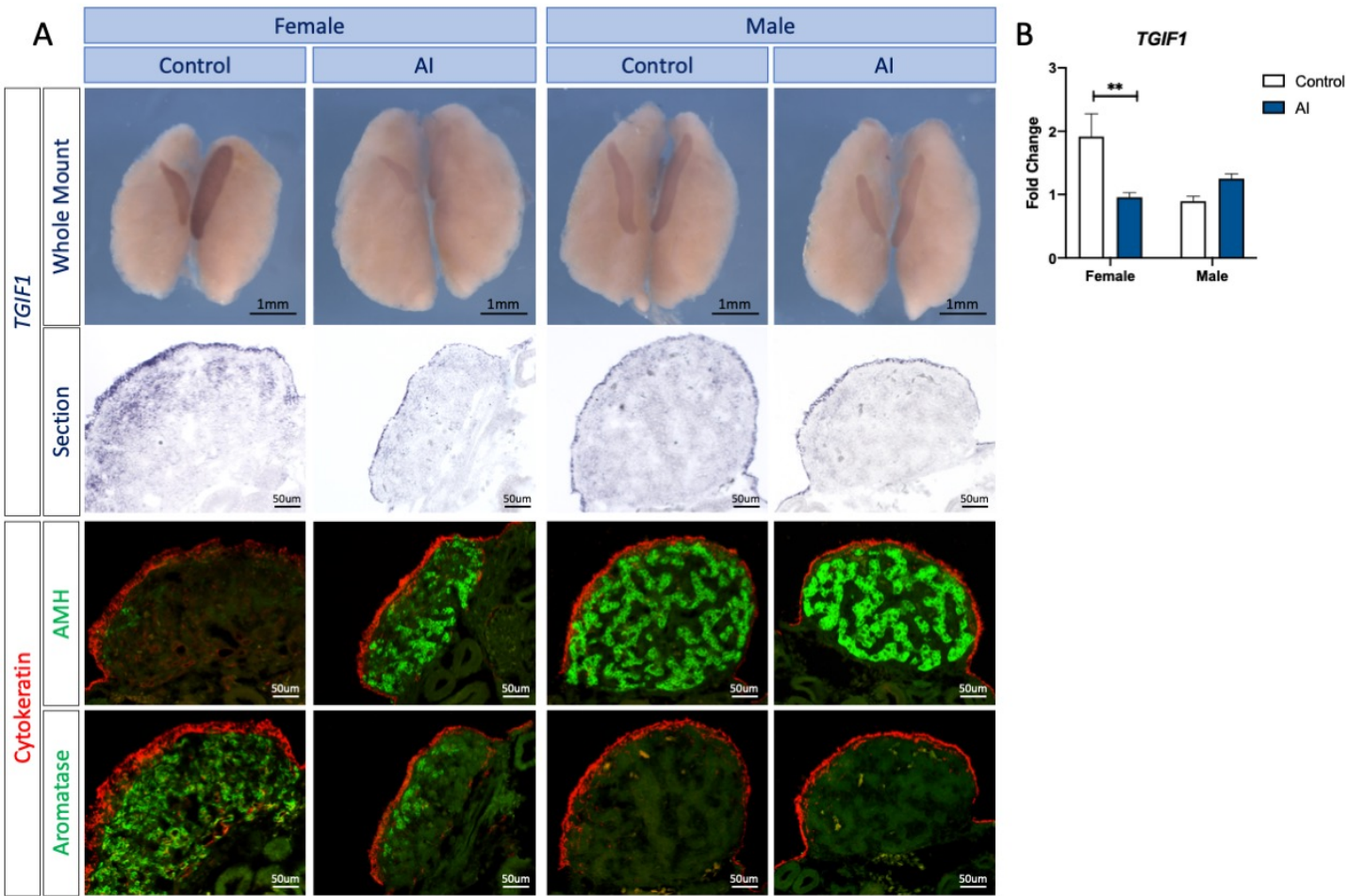
977

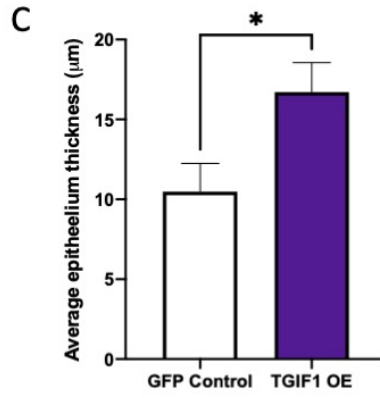
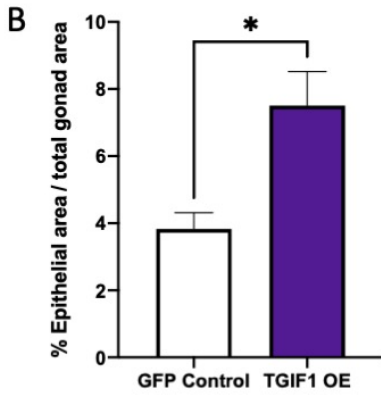
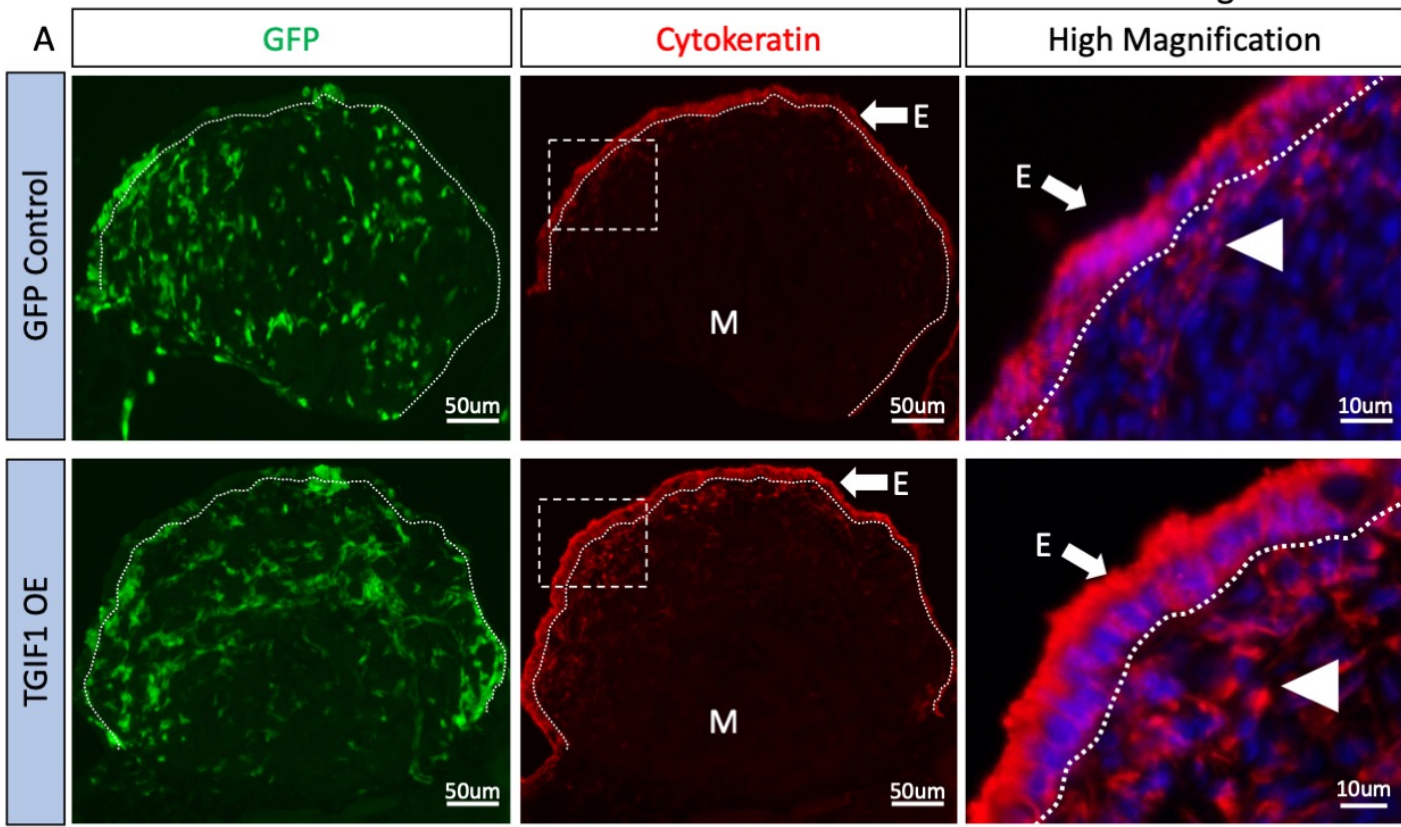
978 **Fig. 10. Role of TGIF1 in epithelial maintenance and juxtacortical medulla formation.** In
979 chicken ovaries (top), the activation of the ER- α signaling pathway by estrogens induces the
980 expression of TGF1 in the gonadal epithelium, resulting in the epithelial structure maintenance
981 and the formation of the juxtacortical medulla by increased epithelial to mesenchyme transition
982 (EMT). In chicken testis (bottom), TGIF1 expression is not induced in the gonadal epithelial cells
983 due to the lack of ER- α signaling. This results in the epithelial flattening and the lack juxtacortical
984 medulla formation.











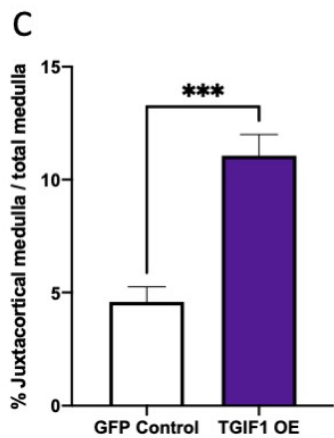
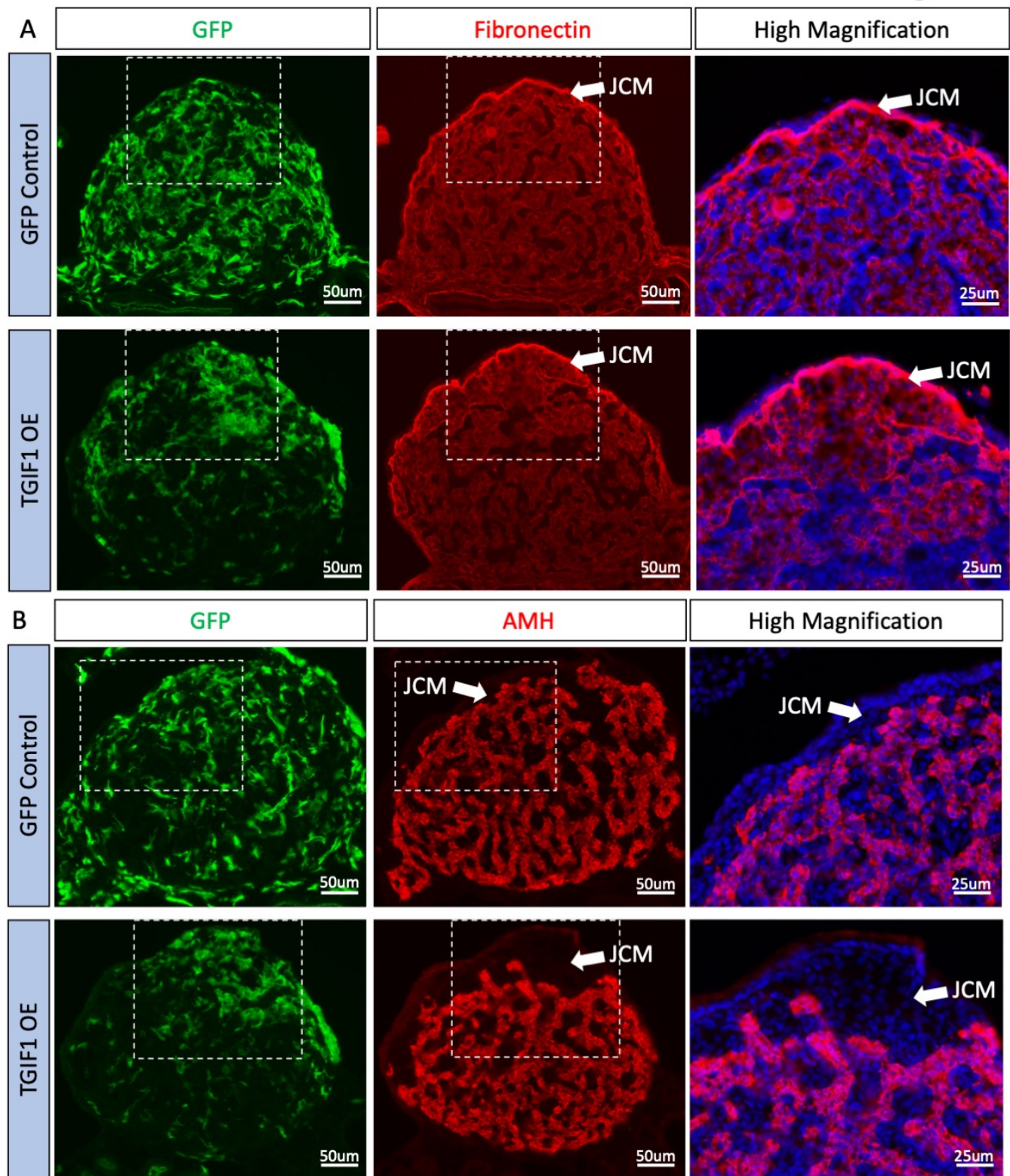


Fig 7

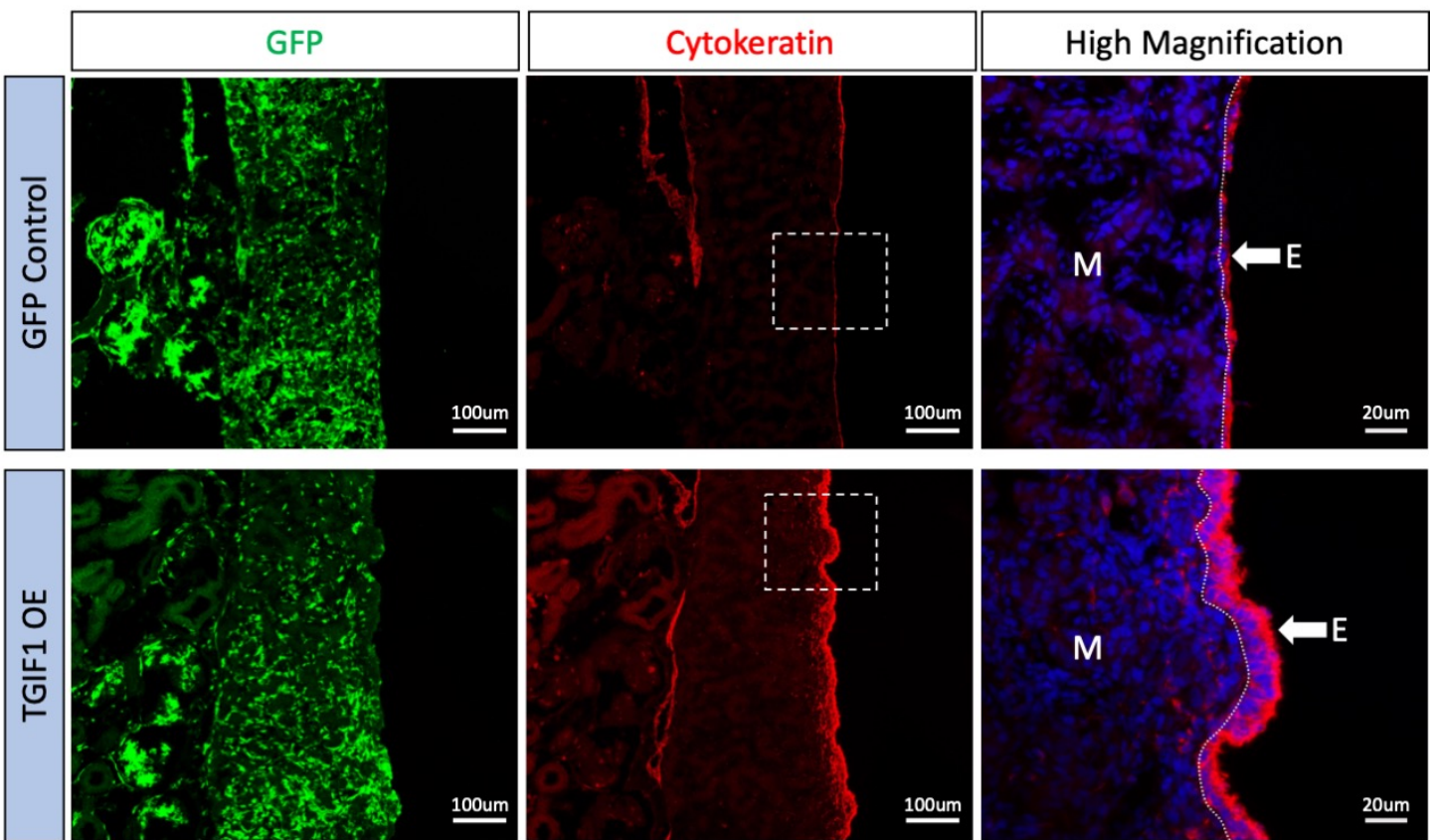


Fig 8

